Detection of Microcracks in Concrete Cured at Elevated Temperature

Final Report

Submitted to

Florida Department of Transportation
(Contract No. BD 545 - 50)

BY

Abdol R. Chini and Enrique J. Villavicencio

M.E. Rinker, Sr. School of Building Construction
University of Florida
Gainesville, FL 32611

July 2006

Detection of Microcracks in Concrete Cured at Elevated Temperature

This report is prepared in cooperation with the State of Florida Department of Transportation

The opinions, findings and conclusions expressed in this report are those of the authors and not necessarily those of the State of Florida Department of Transportation

1. Report No.	2. Government Accession No.	3. Recipient's Catalog No.

4. Title and Subtitle	5. Report Date
Detection of Microcracks in Concrete Cured at Elevated Temperature	April 14, 2006
	6. Performing Organization Code

7. Author's	8. Performing Organization Report No.
Abdol R. Chini and Enrique J. Villavicencio	

9. Performing Organization Name and Address	10. Work Unit (TRAIS)
M.E. Rinker, Sr. School of Building Construction University of Florida Rinker Hall Room 304, PO Box 115703 Gainesville, FL 32611	11. Contract or Grant No. BD 545

12. Sponsoring Agency Name and Address	13. Type of Report and Period Covered
Florida Department of Transportation 605 Suwannee Street Tallahassee, FL 32399-0450	Draft Final (March 28, 2005 – April 30, 2006)
	14. Sponsoring Agency Code

15. Supplementary Notes

Prepared in cooperation with the U.S. Department of Transportation.

16. Abstract

The Florida Department of Transportation specifies a maximum differential temperature of 35°F, between the exterior and interior portions of the mass concrete elements during curing. However, the specification does not specify a maximum curing temperature or a maximum placing temperature. The FDOT mass concrete projects of the past reveal that the temperature of the core may reach up to 190°F to 200°F. The objective of this research project was to determine if high temperature levels during curing of concrete cause microcracks in the concrete matrix. A literature review was conducted to identify industry practices for sample preparation in microscopy analysis. The literature review showed that there are no standard techniques for sample preparation for the intent of analyzing microcracks in concrete with complete assurance that the procedure does not induce secondary cracking. The *in-situ* study of concrete microstructure is an area of great debate because of physical constraints in the cutting and grinding preparation process. However, it was estimated that the preparation procedures used for this study represented the most suitable process given the constraints in time, budget and equipment availability. The specimens selected for the study were chosen from the batch of concrete mixes which produced the highest levels of heat of hydration as well as the highest total temperature levels during curing. Two sets of samples were paired for comparison of temperature conditions during curing. For each sample cured at high temperature, a regular temperature sample was also prepared as a control specimen. The percentage of cracks in each sample, high temperature, and regular temperature for the same concrete sample mix were then compared for microcrack concentration. The procedure for sample preparation was tested against a crack-induced set of samples to validate the sample preparation technique. The samples with induced drying shrinkage cracks displayed approximately 86% more cracks than the non-dried samples. The research revealed that no correlation exists between concrete curing temperature and the concentration of microcracks in the concrete. The data obtained demonstrated no significant difference between the average crack densities for room temperature cured samples and the high temperature cured samples. Therefore, based on the findings of this research it can be concluded that for the samples tested in this experiment the temperature levels reached during mass concrete curing did not influence the formation of microcracks in the concrete structure.

17. Key Words	18. Distribution Statement
Mass Concrete, High Curing Temperature, Microcracks, Scanning Electron Microscopy	No restriction This report is available to the public through the National Technical Information Service, Springfield, VA 22161

19. Security Classif. (of this report)	20. Security Classif. (of this page)	21. No. of Pages	22. Price
Unclassified	Unclassified		

ACKNOWLEDGEMENTS

The research reported here was sponsored by the Florida Department of Transportation. Sincere thanks are due to Mike Bergin, P.E., State Structural Materials Engineer, State Materials Office, Gainesville, Florida, for his guidance, support, and encouragement. Special thanks to Charles Ishee, Structural Materials Engineer, State Materials Office, Gainesville, Florida, for his guidance and contribution during the course of the project and for his helpful suggestions. Sincere appreciation is due to the FDOT State Materials Office Concrete Lab employee in Gainesville, Richard DeLorenzo, for his guidance and help in sample preparation. The authors are thankful to Tanya Riedhammer, Assistant In Engineering at the Advanced Material Characteristic Lab of the University of Florida's Department of Civil and Coastal Engineering who performed the image acquisition of concrete samples using the variable pressure Scanning Electron Microscope (SEM).

TABLE OF CONTENTS

LIST OF TABLES

Tables **Page**

LIST OF FIGURES

Figures **Page**

CHAPTER 1

INTRODUCTION

The American Concrete Institute (ACI) defines mass concrete as "any volume of concrete with dimensions large enough to require that measures be taken to cope with generation of heat from hydration of the cement and attendant volume change to minimize cracking." (ACI 116R - 2003, p.17). By FDOT specifications, during mass concrete pours the contractor must ensure that the temperature differential between the core of the concrete structure and its surface not exceed 35°F (20°C). The increased levels of heat experienced during curing may be caused by several factors: concrete mix material properties (such as heat of hydration), ambient temperature conditions at the time of placement, and core temperature conditions during curing. What this study intends to investigate is the effects of elevated curing temperatures in the development of microcracks in mass concrete.

Temperature differentials from core to surface lead to the generation of thermal and shrinkage cracks; however it has not been determined if high temperature conditions at curing alone can cause the development of microcracks. These cracks like any other crack propagation may eventually cause loss of structural integrity and shortening of service life.

Mass concrete practices were largely developed from concrete dam construction where temperature-related cracking was first identified. Temperature-related cracking has also been experienced in other thick-section concrete structures, including mat foundations, pile caps, bridge piers, thick walls, and tunnel linings. Cracks in any direction in any type of building material regardless of its dimensions signifies volume

change in the material. In the case that the volume change is sufficient to produce cracks of appreciable width, the structural integrity of the material in question may be seriously affected.

Cracking can result from material causes or structural causes, or both. This study will analyze the crack behavior in the microstructure of concrete and the impact of high temperature at curing on crack formation. Material-induced cracks can result from drying shrinkage or thermal cracking. Random cracking from material-related causes can pass through a massive concrete element and the crack widths can vary from hairline to wide (ACI 224R-01, 2001). Hairline cracks inside the structure cannot be identified until they propagate later in the life of the concrete.

Microstructure cracks generated during curing of concrete samples at elevated temperatures will be studied in this project. It is clear that the generation of microcracks presents an area of concern to engineers and contractors building these mass concrete structures. An adverse effect of high temperature levels at curing may be the formation of additional cracks once the concrete is fully hardened. In order to test for this behavior, a simulation where concrete is maintained at an elevated curing temperature, without temperature gradients, must be created.

As specified by ACI, the reduction in temperature of mass concrete between the surface and interior must be limited to the temperature differential dictated by the tensile strength of the concrete at that age (ACI 224.1R-01, 2001). The Florida Department of Transportation (FDOT) requires thermal control plans to maintain temperature differentials of 35°F (20°C) or less between the core and the surface. However, the FDOT has not set a maximum curing temperature requirement for the mass concrete.

This presents the following problem: Does concrete cured at high temperatures, for example between 180°F to 200°F, experience crack formation? If this proved to be true, then maximum temperature requirements would need to be specified in order to control cracking.

In order to determine the effects of curing temperature on concrete microstructure, concrete samples must be prepared and observed utilizing microscopy techniques. Microcrack concentrations for samples cured at room temperature and high temperature conditions must be compared and contrasted. In a study conducted at the University of Florida, "Adiabatic Temperature Rise in Mass Concrete" (Chini and Parham, 2004), concrete samples were prepared using different mix designs, placing temperatures, and curing temperatures. Several concrete samples were cured in heating chambers that simulated the core conditions of mass concrete. Meanwhile, a second set of samples made from the same mix designs were cured under room temperature conditions. A selection of these samples will be used in this study to test for microcrack formation.

The first step in performing this study will be to select two sets of samples, one from the mix design that experienced the highest curing temperature conditions and the other from the mixes that had normal curing temperatures. The samples will then be cut, embedded in epoxy, ground and polished for microscopic analysis. The images generated from the microscope will be analyzed for detection of microcracks and quantified to determine the density of cracks in the concrete. The density values will be examined to determine if they vary depending on temperature conditions.

One of the challenges presented by this project is to establish a sample preparation method that will yield the closest approximation to the natural conditions of

mass concrete at its core without introduction of secondary microcracks and excessive experimental error. The concrete will be analyzed under the assumption that the conditions found in the imaging will be representative of the *in situ* conditions of the concrete. Several sample preparation techniques use in the materials microscopy industry will be considered. Upon choosing the most appropriate technique for our study, the technique will be utilized for sample preparation.

Another challenge of this study is to establish a process for quantifying cracks in the sampled images. Computer applications used for the analysis of electronic images will be used in this project. Once all images are acquired it is imperative that a proper quantification process be developed. Finally, once all data are obtained a statistical analysis will be performed to determine if the results vary significantly for the two sample types.

Considering that internal temperatures ranging from 180°F to 200°F have been recorded in FDOT projects, it is prudent to consider the possible adverse effects that high curing temperature can have on mass concrete structures. Accordingly, the research conducted in this study will evaluate microcracking as a possible effect. The objective of this study is to determine if concrete cured at elevated temperatures, similar to the conditions of a mass concrete structure, generate additional microcracks due to the high temperature conditions experienced during curing.

CHAPTER 2

LITERATURE REVIEW

Presence of voids, cracks, and other defects play an important role in determining the mechanical performance of the concrete. If a concrete surface is pre-damaged by microcrack formation in the near-surface area and exposed to open weathering, capillary effect would increase the transfer of substances from the environment and increase the concrete volume which can lead to several mechanisms capable of negatively influencing durability of the concrete.

Studies have indicated that the development of cracks and connected crack network contributes to the increase in permeability and diffusivity of concrete. The presence of preexisting microcracks of 10 μm or greater on the surface can lead to reduced durability, especially of exposed outdoor structures such as bridge superstructures but also concrete pavements and structures in direct contact with the ground. Patel et al., (1995) found that concretes cured at higher temperatures exhibited a coarser microstructure than that of a typical concrete cured at 32°F (20°C), particularly with respect to ettringite. The presence of microcracks will increase moisture mobility within the concrete, which may produce density gradients within the matrix leading to further microcracking. The domination of the matrix by a network of microcracks is also conducive to the formation of secondary ettringite.

Recorded curing temperature of 180°F to 200°F inside the core of FDOT Mass concrete elements has raised concerns over the initiation of microcracks. Slate and Hover

(1984) defined microcracks as cracks having a width of less than 100 μm, while Jansen defined microcracks as extended faults with a width of less than 10 μm. According to Kjellsen and Jennings (1996), these differences in definition appeared to be closely related to experimental techniques and to the orientation of the studies. For the scope of this study, reasonable and practical interpretations of microcracks were set as cracks having widths less then 10 μm. While macrostructure of concrete can be seen unaided, microstructure (200 μm or smaller) must be observed with the aid of a microscope. It would be fair to say, as the documented research indicates, that cracks and crack propagation is understood well from the macroscopic point of view but unavailability of precise specimen preparation techniques hinder studies of concrete microstructure.

Overview of Sample Preparation Techniques

Sample preparation is a key to microscopic analysis of concrete. Proper preparation of concrete samples so that microcracks and voids develop a distinct contrast against the body of concrete is a pre-requisite for the application of the modern day image processing and analyzing techniques (Soroushian et al., 2003). Poor preparation methods can lead to erroneous diagnoses of problems associated with a concrete specimen. According to Hornain et al., (1996), ideal specimen preparation techniques should not induce any cracks during the preparation of samples, thus techniques which involves prior drying of specimen should not be used. The ideal specimen preparation should be simple, economic, rapid, and should be able to detect very fine cracks. And finally, a sample preparation technique will not be useful without accurate image analysis and processing techniques. The sample preparation would also depend on the type of

equipment used for image collection, required resolution of the image, and objective of the study.

For the past few decades, studies have been performed to find a method which fulfills all definitions for the ideal specimen preparation technique. New equipments and methods developed by technological advances have helped researchers in their analysis of concrete specimens. As reported by Ringot and Bascoul (2001), two methods are necessary for the characterization of microcracks, one for sample preparation and one for quantification of cracks. Sample preparation techniques also depend on the type of microscopy used (S. Marusin, 1995). Acoustic method, ultra sonic and laser sparkle methods are useful for studies related to crack propagations but they are unequipped to monitor initial state of samples' crack quantification. Thus, the rest of the sample preparation techniques can be briefly classified in three main categories: radiography techniques, replica techniques, and impregnation techniques.

Radiography and Acoustic Techniques

Earlier methods by Slate and Olsefski (1963) described the use of X-radiography to study the internal features of concrete and the crack formation process of the mortar and concrete sample. Thin samples of 0.15 in (4 mm) thickness were exposed to X-rays flux normal to the plane of the sample. Cracks were identified from the normal constituent of concrete as penetration of X-rays was greater in the surrounding area. A comparative study carried out by Najjar et al., (1986) indicated that due to poor resolution of images, X-radiography systematically overlooks thin cracks. Neutron radiography described by Samaha and Hover (1992), which is principally quite similar to the X-ray

radiography approach, is in fact a better alternative for increasing image resolution. However, in this process the samples need to be air dried beforehand in order to impregnate the specimen with gadolinium nitrate, which in turn might induce microcracks in samples.

Replica Technique

The replica method developed by Ollivier in 1985 is one of the methods which does not require any pre drying of the sample. In this method, the film of acetylcellulose is placed on the concrete specimen by methyl acetate. The film is taken off after the solvent (methyl acetate) is evaporated in air and observed under the optical or scanning electron microscope. As there is no disturbance made to the specimen surface itself, crack propagation studies can be carried out with the replica method. However, in order to peel the acetylcellulose film safely, the area of film has to be limited to 0.31 in^2 (2 cm^2). Thus too many replicas need to be prepared for covering a significant portion of specimen, which could be time consuming.

Impregnation Techniques

Impregnation techniques are one of the oldest techniques used to study the microstructure of concrete. In this method, concrete samples are impregnated with dye or epoxy to facilitate detection and identification of cracks. In order to reduce difficulty in viewing cracks in dense microstructure, fluorescent dye was used by Knab et al., (1984). However, pre drying of the specimen in an electric oven before impregnation, which could alter the specimen condition, remained a major inhibition to this process. Methods developed by Struble et al., (1989) and Gran (1995) overcome drying of the specimen by

using counter diffusion method for replacement of pore water by a dye-impregnated organic solution. In this method, a thin sample of 0.6 in (15 mm) was cut and kept in solution made by dissolved dye and ethanol. After 4 days of the counter diffusion process between pore water present in concrete specimen and dye-induced ethanol, the specimen was taken out of the solution to remove by polishing the excess dye present on the surface. However, this process could take several days and increases the duration of the test.

Dye impregnation methods

Hornain et al., (1996) modified dye impregnation techniques to reduce the time taken to prepare the specimen. In this Method, 0.009 lb (4 g) of a water-soluble red powder, commercially known as Irgacete, was dissolved in 0.22 lb (100 g) ethanol solution. After keeping specimens for 5 minutes in the dyed solution, a second impregnation was done. After completing these 2 steps, the specimen was taken out and polished under water with 6 μm diamond paste to remove excess dye. In order to achieve proper polishing, the specimen was again polished with 3μm and 1 μm of diamond paste. The polished specimens were observed under the optical microscope at 100X. The study reported that cracks of 1 μm width and less could be easily distinguishable, providing a contrast level between specimen and cracks. During sample microscopic studies, cracks going through the hydrated cement phase were distinguished from discontinuity at the paste-aggregate interface. However, the author reported that the dye impregnation method was not useful in finding cracks in highly porous areas.

Epoxy impregnation techniques

Struble and Stutzman (1989) developed a new technique which involved a three-step procedure to replace pore water from a concrete sample. Epoxy impregnation would not only support the microstructure of the specimen by filling the voids and cracks on curing, but also support fragile pores and matrix phases by restraining it against disintegration during the different stages of preparation. This could be a major issue if the samples are to be viewed under a scanning electron microscope which would generate high pressure inside the chamber. Another advantage of using epoxy is to enhance contrast between the pores, hydration products, and cementitious material. The selection of the type of epoxy depends on the objective of the study. Low viscous epoxy was used for relatively highly permeable materials or cementitious powders, while ultra low viscosity epoxy aids in rapid infiltration for less permeable cement pastes and concrete samples.

The first step for this sample preparation method was to cut the specimen of 1 inch size and immerse specimen in ethanol solution at 140°F (60°C). The blades of the saw were immersed in propylene glycol to prevent it from drying. A companion specimen was prepared by Struble and Stutzman (1989) which was kept in an ethanol solution with red dye to see the extent of time taken for the replacement of ethanol in pore structure. For a given concrete sample, the time taken for replacement depends essentially on the thickness of the sample. After 50% of alcohol replacement in depth by visual inspection in the companion specimen, the solution is replaced by epoxy at room temperature and cured according to the manufacture's specifications. After proper curing, the samples were polished and lapped with abrasion papers and diamond paste in

decreasing order and viewed under the Backscattered Electron imaging technique of the Scanning Electron Microscope.

The samples should be ground and polished perfectly in order to remove raw saw cuts on the specimen. Insufficient polishing would leave a disturbed surface on the specimen and the cracks would not be easily discernible during the microscopic observations. On the other hand, an excessive polishing would contribute to the removal of microstructur and could affect the subsequent quantification operations. It was believed that a higher heating temperature would hasten the process of pore replacement. Higher temperature for heating was not used in subsequent studies due to the limited measurement of quantifying the pore water – alcohol exchange and quick evaporation of alcohol. The modified epoxy impregnation method does not require any heating or vacuum on samples and would not induce any specimen preparation related to microcracks.

However, as reported by Soroushian (2003), epoxy impregnation can highlight more porous areas of cement paste, but generally they do not yield crisp boundaries and sharp contrast between microcracks and air voids against the body of concrete. A new two-stage technique was developed as Ink-Epoxy Impregnation. In the first stage, fine capillary pores were first impregnated with parker blue ink and in the second stage, microcracks and voids were impregnated with fluorescent ultra low viscosity epoxy solution. The specimen were cut to 0.8 – 1.2 in (20 - 30 mm), and lapped by abrasive liquid under 3 PSI pressure After cleaning the specimens for loose debris by first rinsing with water and then in ultrasonic bath, the specimens were dried at 140° F (60°C) for 3-4 hours. Ink impregnation for the first stage was done by keeping the container with ink

and specimen under nitrogen pressure at 280 psi for 18-24 hours. The specimen was removed and heated at 140° F (60°C) for 24 hours to let the ink dry.

Stage 2 was performed for fluorescent epoxy penetration in samples. The samples were kept in a vacuum chamber with 0.38 psi for 1 hour. The epoxy solution was mixed, poured in a glass container, and kept in nitrogen pressure of 0.0133 psi for 3-4 hours. To cure epoxy, samples were heated in an electric oven at 150 °F (66°C) for 18-24 hours followed by polishing operations. When compared with the normal epoxy replacement technique, the ink-epoxy replacement technique gives better results. However, the application of heat as well as vacuum pressure could instigate microcracks in samples.

Thin samples

A study conducted by Anderson (1989) introduced preparing thin sections of concrete samples. In this method, a larger sample of 1.8 in x 1.1 in x 0.8 in (45 mm x 30 mm x 20 mm) was cut from a section of concrete, selected from the portion which was a few inches away from the area to be investigated. The cut section was kept under ethanol for 12 hours to reduce its tendency for cracking. The concrete specimen was kept in a vacuum oven at 85 °F to 90 °F (30°C 32°C) to dry for two hours. A homogenized mixture of low viscosity epoxy prepared with 1.1% by volume of dye was mixed in a magnetic stirrer for 24 hours in advance. The dried concrete specimen was kept in the epoxy solution for 1 hour for vacuum impregnation. It was observed that concrete was impregnated 0.04 – 0.08 in (1-2 mm) in depth. Stage 2 covered the mounting of a glass slide onto the selected face of the specimen with Ultraviolet (UV) hardening glue. The specimen was then ground by a 15-20 μm diamond disc in order to achieve a smooth surface. After the specimen was cleaned and dried, it was re-impregnated with epoxy.

After the specimen was cured, a thin sample was cut from it by a diamond saw and the final grinding and polishing was done. Although the results from this method are widely used in European countries, lengthy sample preparation time and dependability on a skilled and experienced technician are primary requirements.

Impregnation by Wood's metal

Nemati (1997) developed a new approach in impregnation techniques using wood's metal instead of epoxy. The idea of this research was to preserve the microstructure of the concrete samples which are kept under compressive stress to analyze microcracks as they exist under loading. In this three-phased study, cracks were introduced in the concrete specimen by a new test setup which allowed the application of axial stress on concrete and impregnation by Wood's metal simultaneously. Wood's metal was impregnated within the sample for providing stability and better contrast for the identification of microcracks. However, the sample preparation method involved drying of the concrete cylinder at 109.5°F (43°C), as well as gradual heating of test assembly at 122°F (50°C), 167°F (75°C), and 204.6°F (96°C) for unified initiation of molten's metal in the specimen. As explained earlier, heating or drying operations before impregnation could introduce microcracks in concrete. The author reported that in a no load condition, few cracks were observed which could be present due to cracks introduced in sample preparation or drying shrinkage.

Wood's Metal impregnation technique was further developed by Soroshian et al., (2003) for concrete samples without initiating microcracks through stress introduction. In this method, 2 inch (50 mm) thick slices were cut and washed to remove any loose debris

attached. The cleaned sample was kept in an electrical oven at 150 °F (65°C) for 24 hours to remove water present. The dried sample was then kept in a steel mold for impregnation with Wood's metal. To facilitate impregnation and liquidification of Wood's metal, the steel mold was kept inside a vacuum pressure chamber by 0.95 psi for 30 - 40 minutes. After keeping the oven temperature at 200 °F (93°C) for 1-2 hour, the air vacuum was replaced by nitrogen pressure of 280 - 300 psi for 3-4 hours. The specimen was allowed to cool down, followed by cutting a 6 mm sample and then the surface was prepared for viewing under the Backscattered technique in the Environmental Scanning Electron Microscope (ESEM). Results indicated replacement by Wood's metal gave desired contract for microcrack identification against the concrete surface. However, heating and vacuum pressure application on concrete would develop additional microcracks which can be quantified with the original microcracks.

High pressure epoxy impregnation technique

Chen (2002) applied high pressure of > 20 bars to florescent epoxy impregnation in a concrete sample. Samples of 0.8 x 0.8 x 0.6 in (2 x 2 x 1.5 cm) were prepared and after initial drying at 176 °F (80°C) for 2 days, samples were kept in a steel cylinder in epoxy resin at least 2 in (5 cm) higher than the top surface of the specimen. The top and bottom of the steel cylinder were blocked by Teflon, the desired pressure (145,725, 1160, 1450, 2900 & 5800 psi) was applied on the blocks through a hydraulic piston and held under pressure for 90 minutes followed by curing of epoxy by heating it up to 122°F (50°C) for 24 hours. This robust impregnation procedure results in a uniform and vast distribution procedure of the florescent epoxy resin throughout the material structure. Prepared samples were viewed under the optical microscope using UV light. The

experiment proved high pressure impregnation to be a more effective and faster method to induct epoxy resin in cementitious materials. This method shows higher brightness and more effective penetration of epoxy in material; and when pressure and vacuum impregnated samples had been kept in an optical microscope to analyze, the high pressure impregnated samples took less time for reaching a threshold value of photon. Pressure impregnation allows higher tensile and flexural strength in samples compared to the vacuum process, thus implying greater stability of the cementitious specimen during the preparation phase. However, no reports clearly show or address the issue of the introduction of cracks during sample impregnation.

Comparison of Sample Preparation Techniques

Microscopic image is a combination of original material from which the specimen was taken, cumulative effects of all the procedures required to prepare the specimen for examination, the examination technique itself, and our interpretation of the image. Specimen preparation method depends on the type of microscope used for viewing the specimen. The review of all the above techniques reveals that there is no standard specimen preparation for viewing microcracks in cement and cementitious materials. Almost all researchers identified pre-drying of the specimen as a major source of developing cracks prior to microscopic examination. However, most of the studies dried specimens in order to remove the pore water from concrete to facilitate the introduction of dye, epoxy, or Wood's metal. While some techniques required a polished concrete section or broken fracture surfaces, some required thin sections dried at 122 °F (50°C) or oven dried in the NO_2 atmosphere. Some samples were cut with a diamond impregnated wire saw without a coolant, while some samples prepared by epoxy impregnated were cut

by diamond grit or lapped by alumina grit and then polished by diamond grit/ abrasive liquid of decreasing order (Marusin S., 1995).

Some researchers believe that the application of improper sample preparation methods would erode and destroy existing microstructure. It can also introduce elements which are not part of the original specimen which would lead to false diagnosis of the damage mechanism. Most of the specimen preparation techniques require that the sample be dried to a certain degree which would affect the pore structure and can induce more microcracks. As reported by Hornain et al., (1996), crack density increases with intensity of drying. Thus such methods would not be able to give true quantitative analysis of microcracks. Vacuum impregnation methods result in excessive drying of the sample and therefore cracks are introduced during sample preparations (Chen 2002). Techniques involving mechanical polishing to produce either a flat surface or thin specimen could be problematic for concrete as different phases of concrete polish at different rates. Similarly putting concrete samples into a vacuum would lead to loss of water and change of structure.

Polishing and lapping operations to smooth the specimen surface would lead to spreading of components over the surface, thus preventing effective use of dot map studies for elements. Polishing would also destroy delayed etterndite crystals and cracks originating from it. While pressure or vacuum would introduce more cracks in the sample, original cracks would heal or widen by epoxy impregnation techniques (Marusin, 1995). However, the sawn and unpolished approach could be better if the study is related to DEF analysis but for proper crack identification and quantification, sample preparation techniques would be required.

In brief, Bisschop and Van Mier (2002) and other studies have indicated that the impregnation of the whole sample and then cutting thin samples from fully impregnated samples would introduce less microcracks. Specimen preparation techniques involve cutting, drying, lapping, grinding, and polishing. Improper handling of these operations results in induction of additional microcracks. For the scope of this study, the epoxy impregnation technique developed by Struble and Stutzman (1989) was performed as it did not involve any drying of samples in any form. In this two-stage counter diffusion process, pore water is replaced by ethanol, and ethanol is replaced by epoxy without involvement of preheating or use of pressure techniques.

Microscopic Instruments

Optical Microscope

Optical microscopy is one of the favored techniques for concrete petrography. In this instrument, the image is viewed in full color and generally at a lower magnification, thus making it a more suitable technique for observing features at the millimeter scale and larger. Concrete and cementitious specimens prepared by thin-sectioning and fluorescent microscopy techniques can be viewed under the optical microscope with the use of reflected ultraviolet lights. The image acquisition is done by placing a Tri–CCD camera which is linked to a personal computer acquisition system. However, optical microscopes have shallow depth of field and limited resolution capacity, so a highly smooth and polished surface is required to produce a focused image under this technique. Furthermore, the intensity of the vacuum-impregnated sample is not stable after 2 min of

exposure to UV light, and decreases in a continuous fashion with the elapse of time (Chen 2002).

Scanning Electron Microscope

Scanning Electron Microscopy (SEM)/ x-ray microanalysis is comparatively more useful in studies which investigate quantification of microstructural properties such as microcracks and voids. Scanning electron microscopes have greater depth of field and high spatial resolution which produces focused images of poor specimens and analytical data for elemental composition analysis for the features seen on those images. As scanning electron microscopy and optical microscope petrography are different tools, different sample preparations are used for these different approaches.

As described in Figure 2-1, SEM scans a focused beam of electron across the specimen and measures any of several signals resulting from electron beam interaction with the surface of concrete specimen. Images are monochrome in nature because they reflect the electron or x-ray flux resulting from beam/specimen interaction. Three major types of signals generated as a result are Secondary electrons, backscattered electrons, and X-rays analysis.

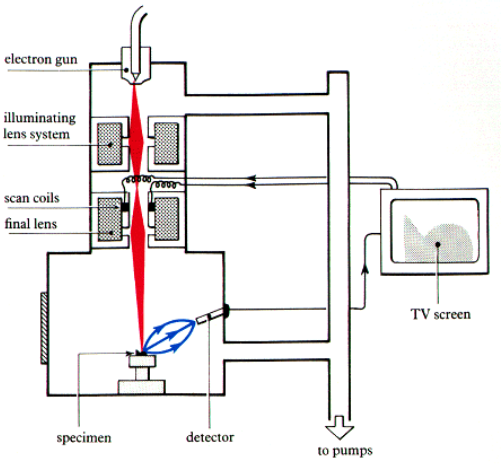

Figure 2-1 Working of Scanning Electron Microscope, (Perkes, 1999)

Secondary Electrons (SE) are low energy electrons resulting from an inelastic collision of a primary beam electron with an electron of a specimen atom. Because of their low energy, they are readily absorbed and only those produced near the surface escape, resulting in an image of surface topography. SE imaging is principally applied in the examination of early age paste microstructure, high magnification imaging of microstructural features, and for examining texture. Knowledge of the morphological and compositional characteristics of the hardened cement paste constituents is invaluable for their identification. As the hardened cement paste matures, filling of the void spaces eliminates the well-formed crystals and backscattered electron and x-ray imaging are more useful in examination of these microstructures (Stutzman, 2001)

Backscattered electrons are high energy beams and capable of reflecting the difference in atomic numbers. They can distinguish between the particles present in a matrix on the basis of the variation in brightness of their images. In the backscattered electron imaging technique contrast is generated by different phase compositions relative to their average atomic number and is observed by differential brightness in the image.

SEM analysis using backscattered electrons and X ray imaging requires a highly polished surface for optimum imaging and X ray microanalysis.

X-ray radiation is produced when a specimen is bombarded by high energy electrons. X-ray microanalysis systems generally employ an energy dispersive detector with the other detector type being a wavelength detector. The x-ray energy level is displaced as the number of counts of each energy interval and appears as a set of peaks on a continuous background. X-ray radiation allows elements of compositions to be obtained as the qualitative analyses print like a dot map image. Each element is identified on a continuous spectrum by the position of its peak.

Any sample can be examined by SE imaging but best use of SE imaging is for examining flat, polished surfaces (Struble and Stutzman, 1989). One of the disadvantages of Scanning Electron Microscopy is that samples must be coated to allow discharge of electron build-up on the examined surface. A thin metal coating decreases build-up of negative charge by forming a conducting path for electrons in order to avoid distorted images. If images are accompanied by X-ray analysis, carbon coating can not be used if a carbonation process is to be studied. A gold coating gives a peak almost at a same position as sulfur (Oberhostler 1992). Thus, in some samples, it might be appropriate to coat the specimen due to concerns for altering the microstructure. High vacuum pressure inside the specimen chamber is also one of the factors which limits the use of SEM as some samples might break or disintegrate under high vacuum pressure.

Variable Pressure Scanning Electron Microscope

Hanke (1999) described many applications where SEM evaluation could be useful to involve samples that are not electrically conductive. These samples have traditionally

required pretreatment, by coating with a conductive film, before SEM examination. Nonconductive samples are subject to a build-up of electrons on the examined surface. This build-up of electrons eventually causes scattering of the incoming electron beam, which interferes with imaging and analysis. Furthermore, samples that contain substantial water or other materials that volatilize in high vacuum also present challenges for SEM examination. These samples require controlled drying to allow the SEM chamber to reach high vacuum and to prevent deformation of the sample at the SEM vacuum.

As the SEM is increasingly used for routine evaluations, there is increasing demand for examination without pretreatment. An answer to the problems of charging and volatile samples is the development of scanning electron microscopes that operate without exposing the sample to high vacuum. These microscopes are referred to alternately as environmental, low-vacuum, or variable-pressure SEM. In variable pressure SEM, the chamber at the electron gun is maintained at high vacuum, while a controlled amount of gas is allowed into the sample chamber. A fine aperture separates the gun and sample chambers to prevent excessive gas entrance into the gun chamber. Separate vacuum systems control the vacuum in the sample chamber and at the gun. The advantages of a higher pressure in the sample chamber are obvious for wet and volatile samples. The higher pressure decreases the rate of volatilization. This decreases the drying and deformation of wet samples.

For nonconductive samples, the advantage of higher pressure is less obvious. When gas molecules in the sample chamber are struck by the electron beam, the gas is ionized. These positive ions are attracted to and neutralize the negative charge build-up on the nonconductive specimens. By controlling the pressure in the sample chamber, the

number of gas molecules intercepting the electron beam is maintained at a level that is sufficient to prevent charging, but does not deflect the beam sufficiently to prevent imaging and microanalysis.

Thus, the use of variable pressure scanning electron microscopes hold advantage over traditional scanning electron microscopes as no coating is required over the samples and samples with moisture could also be imaged.

Image Processing Techniques

Important steps for any microstructural images are to acquire the image and to process the microstructure image to obtain a quantitative analysis of the sample. For this study, quantitative analysis is to identify and measure the number of cracks and crack density over number of images. The image processing should be able to differentiate between voids and cracks, and boundary cracks around aggregates or between phases. Darwin (2001) researched quantification of microcracks of cement mortar samples by the backscatter electron technique of the scanning electron microscope. He reported that the use of edge detection, gradients, and other filters failed to identify cracks passing through low density phases as its intensity depends on adjacent and underlying phases. In his approach, the identification of cracks was based on local changes in grey level. A line scan was taken perpendicular to the images for identification of potential cracks. Perimeter to squared area was taken to differentiate between cracks and voids. Phase identification was also carried out based on pixel intensity. He concluded that as grey level of the image is affected by the density of adjacent and underlying phases, cracks identified based on change in grey level would not be correct. Thus the correct practice

for crack identification should establish minimum gradient in grey level adjacent to cracks.

Soroshian (2003) used segmentation of images from grey level to binary images by using the thresholding approach for viewing microcracks in samples. The research compared manual thresholding operations with three automated thresholding operations such as factorization, entropy, and moment. In manual thresholding, the low threshold level was set to zero or default for auto thresholding and the best threshold level image was determined. The optimum high threshold level was determined by comparing the original gray image and the image after the application of the manual threshold on the binary image. When features of interest (microcracks and voids) were correctly highlighted, the most distant contrast between microcracks/voids and concrete background was obtained. After training the program with images of different resolutions, three automated thresholding operation were performed and results compared with manual thresholding. The study reported that there was no significant difference between the manual thresholding and the automated thresholding operation by the factorization method. There was a difference of 5% and 2% respectively, for entropy and moment methods of the automated process. After identifying the cracks, form/shape factor of 3.5 was used to distinguish cracks from voids. It was shown that the automated process was different by 6.39% and 3.02% from the manual process. However, the author concluded that due to the ease of operation and efficiency given by the automated process, this error was reasonably small.

Summary

The literature review of methods for preparation of concrete samples for viewing microstructure was performed. As described before, many sample preparation methods involved the use of pressure or heat, which might cause concerns over additional cracks in concrete and might lead to erroneous results. Epoxy impregnation of concrete samples was identified as a process which uses a counter diffusion process as sample preparation means for this study. As optical microscope would have inadequate depth of field and resolution for microstructure, scanning electron microscopy was preferred for image acquisition. Variable pressure electron scanning microscope, which requires no special coating over samples but provides ability to view samples with moisture, was found to be more suitable for image analysis. After acquiring images, the manual thresholding approach to mapping microcracks was selected for quantification of microcracks in a given sample.

CHAPTER 3

METHODOLOGY: SAMPLE SELECTION AND PREPARATION

Introduction

In this chapter, the materials and methods used to prepare the concrete samples for microscopic analysis are presented. First, the sample selection criteria are discussed and finally the sample preparation technique described in full detail. The laboratory work was carried out at the University of Florida M.E. Rinker, Sr. School of Building Construction Concrete and Soils Lab. There were two objectives. First, verify the validity of previously applied sample preparation techniques. Secondly, prepare additional samples for image analysis. The methodology is divided into two chapters. The second part, Chapter 4, comprises the procedure for microscopic image acquisition, image analysis, and the quantification of microcracks.

Concrete Sample Selection

The first step was to select the concrete samples that would exhibit the microcrack formation due to high temperature conditions. Samples were selected from the research project, "Adiabatic Temperature Rise in Mass Concrete in Florida," conducted by the University of Florida for the Florida Department of Transportation (Chini et al, 2004). The authors prepared twenty different mixes using AASHTO Type II cement manufactured by two different companies, each with different combinations of cementitious materials and placing temperatures of 73°F (23°C) and 95°F (35°C). The authors studied the effect of the physical properties of the various mix designs with

respect to the adiabatic temperature rise of concrete during curing. For purposes of this study the samples with the worst case scenario properties for high curing temperature conditions were selected.

Since higher placing temperatures result in increased curing temperatures, samples made from the higher of the two placing temperatures (95°F) were selected for microcrack analysis. The field of investigation was further narrowed by selecting the mix made with the cement that had the highest heat of hydration characteristics. A heat of hydration test by Construction Technologies Ltd. revealed higher heat of hydration in AASHTO Type II cement ("Cement B") with 78.2 cal/g at seven days. Meanwhile, the heat of hydration for the other cement, "Cement A", AASHTO Type II cement was 66.2 cal/g at seven days. The combination of these two properties led to the selection of the mixes with Cement B and 95°F placing temperature for this study.

The concrete samples are given mix designations based on their material characteristics. The nomenclature for the mix designations are based on the following properties: Placing temperature, cement type, cementitious material content (expressed in %), and curing temperature. For instance, sample "95B00P-HT" corresponds to a concrete sample placed at 95°F conditions with cement type B, 0% cementitious material (or 100% Portland cement), and cured under sustained high temperature conditions. The concrete samples were prepared using different mixes of assorted cementitious content and were proportioned as shown in Table 3-1.

Table 3-1 Sample mixes and designations

Mix	Placing Temp (^{o}F)	Cement Source	Curing Condition	Sample designation
Type II Portland Cement and 0% Pozzolonic Material	95	B	High Temp	95B00P-HT
			Room Temp	95B00P-RT
80% Type II Portland Cement and 20% Fly Ash	95	B	High Temp	95B20F-HT
			Room Temp	95B20F-RT
65% Type II Portland Cement and 35% Fly Ash	95	B	High Temp	95B35F-HT
			Room Temp	95B35F-RT
50% Type II Portland Cement and 50% Slag	95	B	High Temp	95B50S-HT
			Room Temp	95B50S-RT
30% Type II Portland Cement and 70% Slag	95	B	High Temp	95B70S-HT
			Room Temp	95B70S-RT

The concrete mix samples were kept in two different molds for placing and curing. Samples cured at room temperature conditions were cast in cylinder molds. Meanwhile, the samples cured at high temperature conditions were cast in thermal curing chambers. The thermal curing chambers monitored the curing temperature to maintain an

adiabatic condition. The chambers were connected with thermocouples to a micro-controller that regulated temperature and documented the adiabatic temperature rise during curing. Figure 3-1 shows one of the samples used for this study.

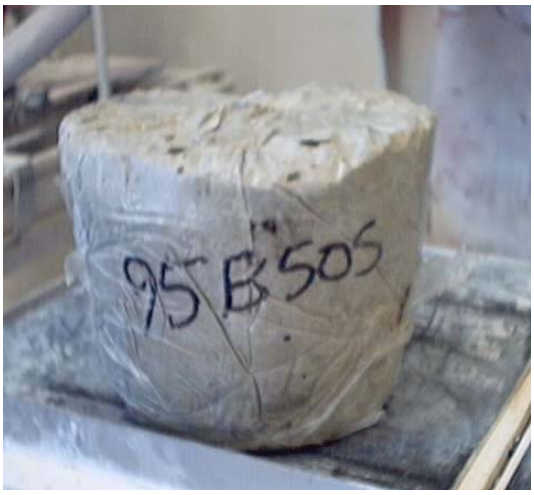

Figure 3-1 Concrete sample

The data provided in Table 3-2 show the temperature rise observed over the first four days of curing in the thermal curing chambers.

Table 3-2 Adiabatic Temperature Rise Data

Cement B (95°F Placing Temperature)					
Time (hrs)	95B00P Temp. Rise (°F)	95B20F Temp. Rise (°F)	95B35F Temp. Rise (°F)	95B50S Temp. Rise (°F)	95B70S Temp. Rise (°F)
0	0.0	0.0	0.0	0.0	0.0
12	2.6	56.8	50.4	58.6	45.0
24	72.2	72.9	61.9	76.7	69.4
36	84.2	77.4	67.9	80.7	73.9
48	85.6	77.6	68.9	81.8	76.3
60	85.7	77.6	69.2	82.0	77.9
72	86.0	77.6	69.3	82.0	78.9
84	86.0	77.6	69.6	82.0	79.5
96	86.0	77.6	69.9	82.0	79.9
Total Temp	181°F	172°F	164°F	177°F	174°F

The temperature data in Table 3-2 indicate sample 95B00P had the highest temperature rise of 86°F over a placing temperature of 95°F, closely followed by 95B50S with a temperature rise of 82°F. The conditions inside the chamber simulate curing temperatures of 181°F and 177°F respectively for mixes 95B00P and 95B50S. The temperatures reached inside the thermal chambers are representative of the conditions found at the core of a mass concrete structure.

The decision to select sample 95B00P was made since it constitutes the worst case scenario of all samples for likelihood of cracking in the concrete microstructure due to high temperature conditions.

Sample Preparation Technique

The method utilized for sample preparation was similar to the epoxy impregnation process performed by Struble and Stutzman (Struble et al., 1989). The process of concrete impregnation with epoxy involves a counter diffusion method wherein the pore water of concrete is replaced with ethyl alcohol and then by a low viscosity epoxy. The method does not require pre-heating of the concrete sample nor does it require applying vacuum pressure for impregnation of the epoxy. What this method provides is a viable economic method with minimum destructive procedures which best suits the needs of this study. The only drawback from this preparation procedure is the heating of the sample during epoxy curing. It was found that in order to ensure polymerization of the epoxy resin the samples had to be heated at 140°F for 12 hour periods. The process of preparing the sample from first cut to final polish is described in detail next.

Procedure for Sample Preparation

The first step was to section pieces of concrete from the samples prepared in the study of "Adiabatic Temperature Rise of Mass Concrete in Florida". Before and after the cutting procedures were performed, all the samples were stored in moist rooms at the

FDOT Materials Lab in Gainesville, Florida. Figure 3-2 shows the samples and diamond saw equipment from the FDOT lab facilities.

Figure 3-2 Diamond blade saw used for first cutting operation

The concrete samples were cut to 1/2" (13 mm) thick pieces with the diamond saw. After that the samples where cut down to squares of 1.5" (38 mm) and 1/4" (6.3 mm) thick. These fine cuts were done with a diamond wafer saw, Trim Saw by Allied High Tech, Inc. shown in Figure 3-3. The cuts were performed at 480 RPM with a 6" (15.24 cm) diameter diamond metal bond blade, 0.02" (0.5mm) thick. The cuts were performed manually and the blade was constantly lubricated with a low speed propylene-glycol based cutting fluid by Allied High Tech, Inc. The cutting fluid is designed exclusively for low speed cutting (<500 RPM) applications where a thicker formula is needed to lubricate blades, remove debris from the cut, and reduce friction.

Figure 3-3 Trim saw

In order to test the sample preparation technique, a set of samples had to be prepared that was pre-heated above 212^{o}F in order to induce microcracking. The two samples that were put to this test were samples 95B00P-RT1 and 95B00P-HT1. The oven-dried samples were labeled 95B00P-ODRT1 and 95B00P-ODHT1. These "preparation technique test samples" were placed in an oven for a period of 12 hours at 250^{o}F and later prepared exactly the same way as the regular non-oven dried samples.

Once the samples were cut down to the desired size, the process of epoxy impregnation began. In this process, the first step was to replace the water in the voids and pores of the concrete with 200% proof ethanol made by Sigma-Aldrich, Inc. The samples were placed in a lidded jar filled with ethanol. A control sample was used to determine the depth of replacement of the pore water with alcohol. The control was a remnant of the original sample after trimming. This remnant was now placed in a jar filled with ethanol and dyed with a red dye by PolyScience, Inc. By sectioning the companion sample after a period of time, the depth of replacement was observed by the

depth of dye coloration. On average, alcohol-pore water replacement was found to be approximately 1mm/day. After three days the control sample was cut and the red coloring showed evidence of the replacement to a noticeable depth (Figure 3-4).

Figure 3-4 Red-dye water-ethanol replacement in control sample

Once the ethanol replacement was complete, the samples were infiltrated with epoxy. The replacement with epoxy was performed as specified by a company representative and the product's manual. The product is an ultra-low viscosity epoxy kit from Structure Probe, Inc. shown in Figure 3-5. The epoxy kit is made up of four chemicals and mixed to obtain the desired quantity as described in Table 3-3.

Figure 3-5 Ultra Low Epoxy Kit

Table 3-3 Mixing Schedule for Epoxy

Name of Chemical	Mixing Schedule
Vinylcyclohexene dioxide (VCD)	0.022 lb (10 g)
n-Octenyl succinic anhydride (n-OSA)	0.044 lb (20 g)
Butanediol Diglycidyl Ether (BDE)	0.0007 lb (0.3 g)
Dimethylaminoethanol (DMAE)	0.0007 lb (0.3 g)

The ultra low viscosity protocol for the infiltration process was performed as follows:

Stage 1: Immerse the samples in a 3:1 ethanol:epoxy mix for 12 hours,

Stage 2: Immerse the samples in a 1:1 ethanol:epoxy mix for 12 hours,

Stage 3: Immerse the samples in a 1:3 ethanol:epoxy mix for 12 hours,

Final stage: Immerse the samples in a 100% epoxy bath for 12 hours.

The challenge with this replacement process was to keep all epoxy stages isolated, as much as possible, from oxygen. The manufacturer's recommendation was to do this in a dry nitrogen environment in a glove bag purged of air, but this was not feasible for this project, given the resources available. Instead, during the mixing and preparation, careful attention was placed to avoiding having air bubbles in the epoxy-ethanol baths. See Figure 3-6 for an example of a sample in an epoxy mold with the un-polymerized epoxy mix after the infiltration process is complete.

Figure 3-6 100% epoxy infiltration with failure to polymerize

For curing of epoxy during all stages of replacement, the samples were kept in an oven at 140°F (Figure 3-7). At the final stage, the samples were ready for the cutting and polishing steps. Grinding and polishing are vital steps in the sample preparation process. Grinding is used to expose a clear surface layer and to remove excessive epoxy coating on the surface. However, excessive grinding could cause damage to the concrete sample

and create secondary cracking. The grinding and polishing processes were done with an MPrep3 Grinder-Polisher Machine by Allied High Tech, Inc. (Figure 3-8).

Figure 3-7 Samples inside oven

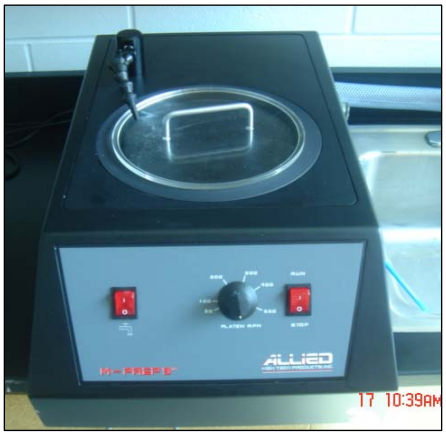

Figure 3-8 MPrep3 grinder and polisher

The grinding and polishing procedure is a multi-step process that involves the use of various materials and techniques that are best described and illustrated in Table 3-4 and Figures 3-9 and 3-10. The process for grinding and polishing was developed in conjunction with the product application specialists from the manufacturer of the consumables and equipment used in this project, Allied High Tech, Inc.

Table 3-4 Grinding and polishing procedure for manual preparation of samples with MPrep3 machine and Allied High Tech, Inc. consumable products

Steps	**1**	**2**	**3**	**4**	**5**	**6**
Abrasive	180 grit	320 grit	600 grit	6 μm	1 μm	0.05 μm
Type	Silicon Carbide Paper	Silicon Carbide Paper	Silicon Carbide Paper	Polycrystalline Diamond	Polycrystalline Diamond	Colloidal Alumina
Carrier	Grinding Disc	Grinding Disc	Grinding Disc	Glycol Suspension	Glycol Suspension	Polishing Suspension
Polishing Cloth	-	-	-	Gold Label™	White Label™	Chem-Pol™
Coolant	Water	Water	GreenLube ™	GreenLube ™	GreenLube ™	GreenLube ™
Platen Speed/ Direction	250 RPM Comp**	250 RPM Comp**	250 RPM Comp**	250 RPM Contra*	250 RPM Contra*	250 RPM Contra*
Pressure	Approx. 8-10 lbs	Approx. 8-10 lbs	Approx. 8-10 lbs	Approx. 10-12 lbs	Approx. 10-12 lbs	Approx. 10-12 lbs
Time	1:30 min	1:00 min	1:00 min	1:30 min	1:30 min	1:00 min
*Contra: Platen and sample rotate opposite direction (clockwise)						
**Comp: Platen and sample rotate in same direction (counterclockwise)						

Figure 3-9 Consumables from Allied High Tech, Inc. used for grinding/polishing

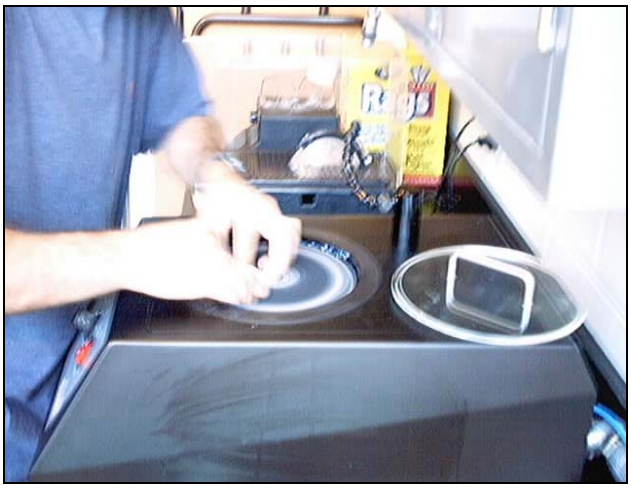

Figure 3-10 Polishing procedure with colloidal alumina in grinder/polisher machine

The polishing was done to remove the surface damage resulting from the sawing and grinding of the sample surface. After grinding at 600 grit, the surface became smooth and ready for further polishing. The polishing operation involves successively decreasing the size of diamond suspension paste from 6µm to 1µm and a final pass with 0.05µm colloidal alumina suspension (Figure 3-10). The polishing provides the

reflectivity of the surface needed to obtain a clearer picture when the sample is scanned under the microscope.

Image Acquisition Sample Preparation

Once the samples were ready for viewing under SEM, a ¼" (6.3 mm) square grid was drawn on them. The grid was created by tracing with an ultra-fine scan marker by Pilot with a 0.015 in (0.4 mm) stroke width, shown in Figure 3-11.

Figure 3-11 Ultra-fine tip scan marker used for creating sample grid

This marker works well with the SEM image acquisition system since it provides a detectable coordinate grid system for identifying the location of each image being scanned. For each of the grid's cells a single image was scanned and analyzed. The samples were turned over to the SEM technician for imaging as seen in Figure 3-12. Notice the reflection obtained from the polishing process. Additionally, Figure 3-12 illustrates the X marks written onto the sample surface to identify the cells which were predominantly aggregate instead of the cement paste areas, which are of most interest for identifying microstructural cracking. The cells marked with an X were not scanned.

Figure 3-12 Finished polished sample

A total of 10 samples similar to the one shown in Figure 3-11 were prepared using the equipment and techniques mentioned in this chapter. In the following chapter the process of image acquisition and image analysis for crack identification and quantification is explained.

Summary

The determination of which sample preparation technique to use was studied based on several factors that influenced the credibility and viability of this study. The sample preparation technique that was used was the epoxy impregnation technique as performed by Stuble and Stuzman (Struble et al., 1989). The following table 3-5 summarizes the sample preparation techniques considered and evaluated based on several characteristic criteria.

Table 3-5 Sample Preparation Methods for Microscopy Analysis of Concrete

Method	ASTM Standard	Exposed Temp.	Exposed Pressure	Costly	Microscopy Equip.	Equip. Available
Epoxy Impregnation	C856	140°F (60°C)	Negligible	No	SEM	Yes
Dye Impregnation	None	Room	Negligible	No	Optical	Yes
Dye & Fluorescent Epoxy Impregnation	C856	140°F (60°C)	280psi Nitrogen	Yes	SEM	Yes
Wood's Metal	None	200°F (93°C)	280psi Nitrogen	Yes	SEM	No
ESEM Method (Humidity control)	None	37°F (3°C)	Water vapor	Yes	ESEM	No
High Pressure Epoxy Impregnation	C856	176°F (80°C)	High	Yes	SEM	No

One of the goals of this research was to test the sample preparation technique for its reliability and possible tampering of concrete samples with the creation of secondary microcracks. Two sets of samples were created where one was oven-dried at 250F and later impregnated with the low viscosity epoxy and the other impregnated without prior cracking by drying.

Additional samples were prepared for image analysis with the goal of determining whether the high temperature curing conditions resulted in increased levels of

microstructural cracking. The sample preparation steps of grinding and polishing were conducted based on the manufacturer's recommendations. It was found that the ultra-low epoxy kit by SPI was not practical in the mixing of the kit components. A recommendation for future studies would be to use an epoxy resin system that consists of only two ingredients, resin and hardener, and can be mixed and cured with greater ease.

CHAPTER 4

METHODOLOGY: IMAGE ACQUISITION AND ANALYSIS

Introduction

In order to properly identify microcracks in the concrete samples an image analysis tool had to be used. In this chapter, the image acquisition and analysis processes are described. The first step in the imaging phase was the image acquisition via Scanning Electron Microscope (SEM). Subsequently, the digital images obtained from SEM were analyzed for microcrack identification and quantification. The challenge of the image analysis process was to find a system that would enable the analysis of numerous images in an automated, timely, and user-friendly manner. The tool had to be able to automatically identify and measure microcracks in the image field. In order to find a product that would enable such an analysis, a market study was performed to find the computer software that would provide the following tools and capabilities:

- Grayscale analysis of samples.
- Manual brightness thresholding
- Crack identification based on size factors
- Filtering of noise and voids.
- Quantification of total crack length in the image area.
- Output of data for statistical analysis.

Each of the images had to be analyzed individually and quantified for total crack length. The data were gathered to calculate the crack density for each image, which was obtained using the following formula:

Crack density = Total crack length (μm)/ Image field area (μm^2)

There were a total of 325 images generated. Each image had an area of 565,500 μm^2 (650μm x 870μm). Table 4-1 shows the list of samples and labels for each of the samples used in this study, as well as the number of images produced per sample.

Table 4-1 Sample and image list

Sample	Number of Images
95B00P HT-1	29
95B00P HT-2	27
95B00P HT-3	30
95B00P RT-1	43
95B00P RT-2	34
95B00P RT-3	21
95B00P ODHT-1	42
95B00P ODHT-2	22
95B00P ODRT-1	43
95B00P ODRT-2	34
Total	325

Each image was labeled with a grid system that was used to identify individual matrix cells and areas of particular interest. The grid system is shown in Figure 4-1.

1	**2**	**3**	**4**	**5**	**6**
7	**8**	**9**	**10**	**11**	**12**
13	**14**	**15**	**16**	**17**	**18**
19	**X**	**20**	**21**	**22**	**23**
24	**25**	**26**	**27**	**28**	**X**
29	**30**	**31**	**32**	**33**	**34**

Figure 4-1 Concrete sample with grid

Image Processing

Image acquisition was performed at the Advanced Material Characteristic Lab of the Department of Civil and Coastal Engineering, University of Florida, Gainesville. The facility houses a Hitachi S-3000N, variable pressure Scanning Electron Microscope (SEM) shown in Figure 4-2.

Figure 4-2 Hitachi S-3000N SEM from the University of Florida Advanced Material Characteristic Lab

This SEM allows for the viewing of the concrete samples without the need to cover the samples with a conductive surface. The samples are highly polished to obtain optimum imaging results. The SEM machine scans a focused beam of electrons across the specimen and measures any of several signals resulting from the electron beam interaction with the surface of the concrete sample. The three major types of signals generated by the SEM are secondary electrons, backscattered electrons, and x-rays. Backscatter electrons are highly energized beams that can be used to distinguish between the particles in the concrete surface on the basis of variation in brightness and grayscale value. As reported by Stutzman (2001), the backscatter electron and x-ray imaging tools

are useful in identifying cracks in the cement paste with grayscale alteration. The images that are generated from the SEM scanning procedure are manipulated to uncover features of interest, such as microcracks and voids.

All SEM images for this study were generated with the following settings:

- Vacuum: 30 Pa (0.24 Torr)
- Accelerating voltage: 15.0 KV
- Scale: 300μm
- Pixel Type: 8-bit grey levels
- Image Size: 1280 x 960 pixels
- Magnification: 150X

The images were all generated with the same scale, pixel type, and magnification level. It was determined that the magnification level of 150X was most suitable for microcrack analysis since it allowed for the identification of cracks of considerable width and length while covering the largest sample field area. Previous work used several magnification levels ranging from 125X to 500X for image analysis (Soroushian et al., 2003). Additionally, the selected image size provided a wide array of aggregate-paste boundary conditions which are of particular interest, such as interfacial transition zone cracking.

Image Analysis and Microcrack Quantification

For this study, the quantitative analysis of the samples consisted of the identification and measurement of the cracks and crack density in the images. Images taken from multiple areas of the concrete matrix and aggregate interfacial transition zone provided information related to the microstructure of the sampled concrete. An automatic mapping of the cracks was done in order to find out the total length of the microcracks and density per image area. The microcracks, voids and noise were distinguished visually, and their corresponding lengths were measured using the image analysis software AxioVision™ version 4.4.1 by Carl Zeiss.

In order to identify microcracks from the image, segmentation techniques were used. Segmentation is a process through which the images are partitioned into meaningful areas based only on the intensity of the pixels. The intensity of each pixel is defined by its grayscale value. Grayscale analysis involves the use of threshold levels for the different grey levels present in the image. This study used 8-bit grey level images which contain grayscale values between 0 and 256. The optimum threshold range was determined by comparing the original image with the resulting highlighted image generated via the manual threshold operation. With the AxioVision™ software the features which fell within the threshold parameters where highlighted in red. The grayscale histogram could be toggled up and down the grayscale values until the features of interest were highlighted (Figure 4-3). As can be seen in Figure 4-3 many of the features that are delineated by the manual thresholding procedure are not microcracks. However, the microcracks are identified and are further filtered out by using the pixel length criteria (Figure 4-4).

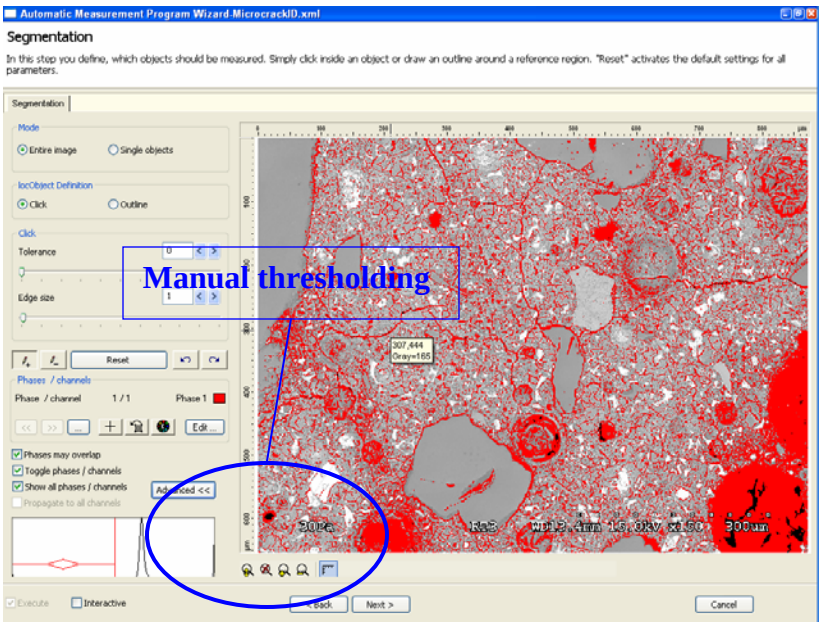

Figure 4-3 Segmentation step from image analysis program

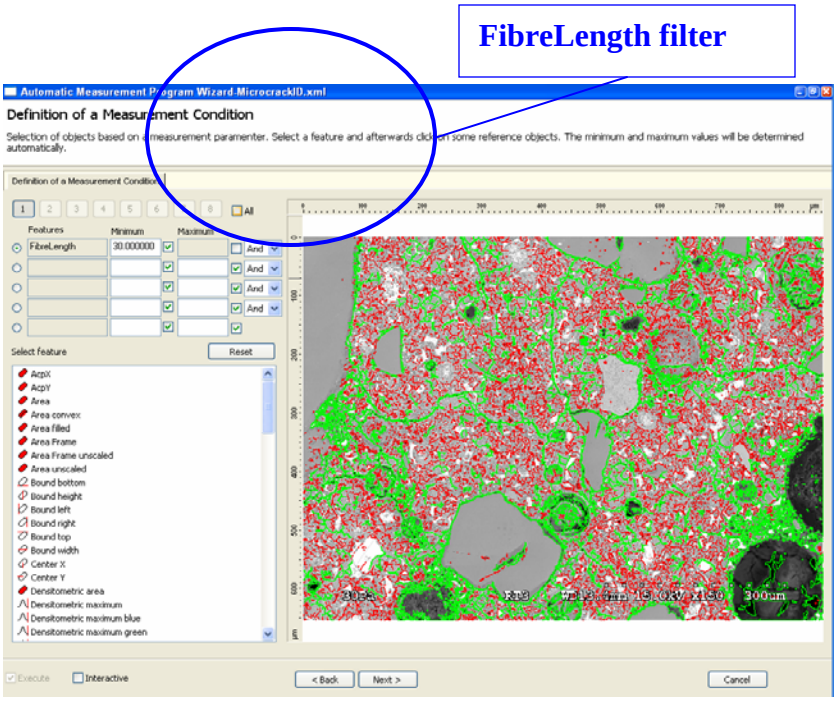

Figure 4-4 Measurement condition filter using FiberLength measuring tool

The software module AutoMeasure™ from the AxioVision program provides a very useful tool in measuring crack length. In order to quantify the cracks the measurement tool FibreLength™ was implemented. The FibreLength measurement allows for the measurement of crack lines that are irregular and curved. It is an algorithm that estimates the length of the fiber-shaped outline of the microcrack or image feature, which can be seen highlighted in green in Figure 4-4.

The pixel length criterion for filtering out noise and other highlighted features of the concrete microstructure was established based on the data provided by Soroushian's study on image analysis for quantification of microcracks (Soroushian, 2003) . Table 4-2, was taken from the research paper as published by Cement and Concrete Research Vol. 33, p. 1960. The equivalent micron lengths were calculated using the scaling feature in AxioVision, where 1 pixel was equal to 0.6818 μm. The equivalent to 40 pixels in length, or 30μm was determined as the threshold for the minimum microcrack length criterion.

Table 4-2 Lengths of noise, microcracks and voids at three different magnification factors

Length (pixels)	125X magnification			250X magnification			500X magnification		
	Noise	Micro - cracks	Voids	Noise	Micro - cracks	Voids	Noise	Micro - cracks	Voids
Min	2	18.4	8	2.82	29	6.72	2	29	35.5
Max	106	478	612	82	756	906	165	948	745
Mean	15.5	97.7	107	16.8	130	205	24.4	198	271

Source: Soroushian et al., " Cement and Concrete Research Volume 33, No.12, Page 1949-1962, December 2003

A sensitivity analysis was performed to determine if this 30 micron length parameter would create a significant change in the results of total crack length and crack density per image. After attempting minimum crack lengths of 10, 20 and 30 microns it was found that the data did not deviate significantly and therefore were not sensitive to the small change in minimum crack length parameter. This can be explained because of the fact that the noise features are generally found in the smaller scale lengths, which can be interpreted from the findings of Soroushian in Table 4-2.

Further filtering of noise could be performed manually to remove features that were highlighted by the program automatically and did not fall out of the threshold parameter for microcrack length. An example of this condition was found on multiple occasions with features that were created artificially like water bubble marks left on the surface. These circular patterns had cracks around their perimeter and created mapped cracking around them. This particular condition was eliminated in every case, since they could be picked out individually and eliminated from the microcrack data set. Figure 4-5 shows a print screen of the program step were the cracks can be individually selected for removal from the data set. The circular areas that were eliminated were either large voids filled with epoxy or water bubble marks as mentioned before. Figures 4-4 and 4-5 show the unselected areas (non-microcracks), in red.

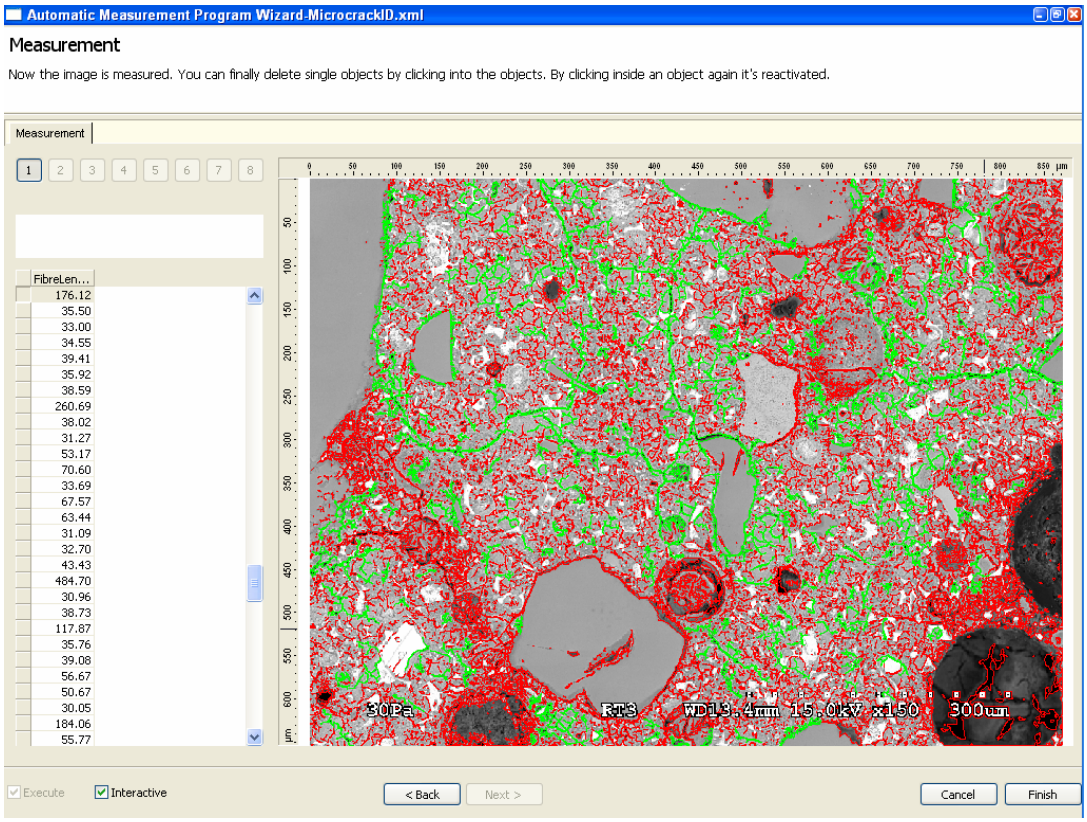

Figure 4-5 Final step in microcrack detection w/ manual selection of cracks/features

The final output of the image analysis software is shown in Figure 4-6. The microcracks highlighted in the image shown are listed in table format by microcrack length. These lengths were gathered for each image and a data table created for each sample. The sum of all microcracks in each image was computed and then the crack density for each image. The results are shown and analyzed in Chapter 5.

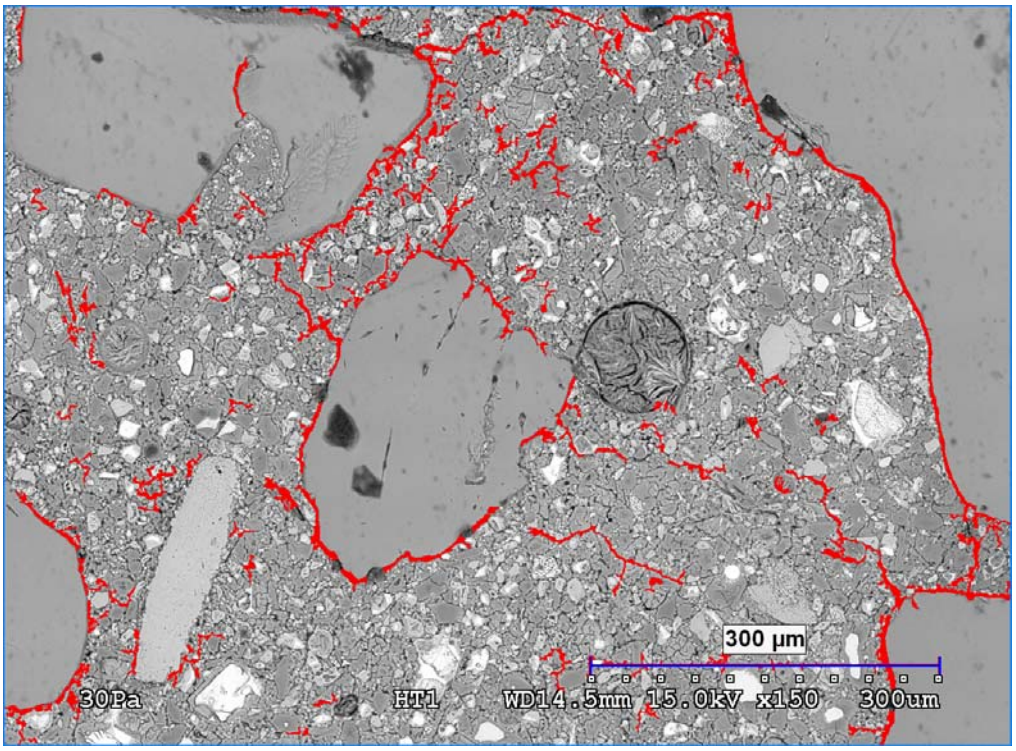

Figure 4-6 Output image from AxioVision software

Summary

Despite all precautions taken during specimen preparation there still exists a large probability that the captured images may contain error from different sources. Such sources of error can be associated with leftover impregnating agent on the surface of the sample, uneven distribution of light under the microscope, improper adjustment of brightness and contrast of the microscope, damaged surfaces from the impregnation and sample preparation process, as well as the visual identification of cracks based on manual thresholding. The microcrack observations in the concrete samples were finally

identified and quantified for analysis of microcrack behavior. The results were gathered in spreadsheet format by the AxioVision program and analyzed using Microsoft Excel.

During image analysis three different software operators analyzed approximately 100 images each. The effects of operator bias were evident. In order to test for operator bias two operators analyzed and quantified the same images and came up with different results. The major difference came from the manual elimination of cracks at the end of the software routine. The differences in crack density values obtained can be interpreted as follows:

1. Improper interpretation of the program segmentation steps
2. Differences in interpretation of the selection criteria for removal of unrepresentative features of microcrack patterns.

Due to time and resource constraints this study took the data sets as generated and quantified the average crack density values for analysis. The conclusion of whether cracks are present in the concrete that was cured at higher curing temperatures was presented based on the test results.

CHAPTER 5

RESULTS

Introduction

In this chapter the results of the microcrack density in concrete samples are summarized and compared for different curing temperature conditions. The data collected consisted of total crack lengths per image for 323 images and 10 samples. The first four samples were prepared with the intention of testing the sample preparation method validity. This was achieved by comparing the results of the crack densities for samples that were pre-dried to induce artificial cracking of concrete versus samples prepared with the same sample preparation technique and mix design but without the pre-drying crack inducement. Finally, additional samples were prepared and analyzed to compare crack density values for samples that were cured at normal temperature conditions and those cured under high temperature conditions. The high temperature conditions are simulating the conditions at the core of a mass concrete structure.

Sample Preparation Procedure Test Results

Results from this study showed that the average crack density of the concrete samples that were pre-dried in an oven to induce microcracks was significantly larger than the density of cracking found in the samples that were not dried. This test was done to prove that the sample preparation technique and images generated were representative of the *in-situ* sample conditions. In other words, what the first part of this study intended

was to show that the process of preparation with epoxy impregnation, lapping, grinding, and polishing, was not tampering with the microstructure of the concrete in a manner that would significantly alter the conditions of the concrete microstructure as found in place. Crack densities for oven-dried samples cured at room temperature and high temperature are shown in Tables 5-1 and 5-2, respectively. Tables 5-3 and 5-4 show crack densities for non oven-dried samples cured at room temperature and high temperature. Figure 5-1 illustrates a comparison between average crack densities of two samples ODRT-1 and RT-1 that are cured at room temperature. It shows that the crack density of the oven-dried sample is 140 percent higher that of the non-dried sample. Figure 5-2 shows that this ratio increases to 160 percent when the samples are cured at high temperature. Table 5-5 and Figure 5-3 show that average crack densities for four oven-dried samples is 86 percent higher than average crack densities for six non-dried samples.

Table 5-1 Microcrack density for oven-dried samples cured at room temperature

	OD RT1	OD RT1	OD RT2	OD RT2
IMAGE #	TOTAL CRACK LENGTH µm	CRACK DENSITY µm/µm^2	TOTAL CRACK LENGTH µm	CRACK DENSITY µm/µm^2
1	16022	2.83%	19063	3.37%
2	14868	2.63%	16995	3.01%
3	14916	2.64%	21693	3.84%
4	11915	2.11%	29034	5.13%
5	12911	2.28%	20954	3.71%
6	13599	2.40%	23184	4.10%
7	17684	3.13%	33687	5.96%
8	6441	1.14%	33461	5.92%
9	19630	3.47%	26790	4.74%
10	17687	3.13%	29313	5.18%
11	16603	2.94%	20390	3.61%
12	16802	2.97%	6132	1.08%
13	16022	2.83%	19063	3.37%
14	14646	2.59%	36788	6.51%
15	7921	1.40%	19582	3.46%
16	15626	2.76%	30207	5.34%
17	10977	1.94%	29701	5.25%
18	5095	0.90%	14721	2.60%
19	8813	1.56%	14493	2.56%
20	8813	1.56%	13286	2.35%
21	7361	1.30%	22469	3.97%
22	6244	1.10%	14026	2.48%
23	18389	3.25%	24782	4.38%
24	9731	1.72%	22514	3.98%
25	13977	2.47%	22008	3.89%
26	9715	1.72%	14588	2.58%
27	14218	2.51%	9631	1.70%
28	12968	2.29%	11222	1.98%
29	5814	1.03%	8364	1.48%
30	6126	1.08%	8676	1.53%
31	9225	1.63%	11467	2.03%
32	13977	2.47%	22008	3.89%
33	5660	1.00%	6730	1.19%
34	9850	1.74%	5882	1.04%
35	4711	0.83%	16521	2.92%
36	6197	1.10%		
AVE		**2.00%**		**3.43%**
STD DEV		**0.75%**		**1.48%**

Table 5-2 Microcrack density for oven-dried samples cured at high temperature

	OD HT1	OD HT1	OD HT2	OD HT2
IMAGE #	TOTAL CRACK LENGTH µm	CRACK DENSITY µm/µm^2	TOTAL CRACK LENGTH µm	CRACK DENSITY µm/µm^2
1	12947	2.29%	13241	2.34%
2	14147	2.50%	28556	5.05%
3	5553	0.98%	21081	3.73%
4	6738	1.19%	13768	2.43%
5	3921	0.69%	N/A	
6	1486	0.26%	15808	2.80%
7	24295	4.30%	23529	4.16%
8	24295	4.30%	24071	4.26%
9	5499	0.97%	35959	6.36%
10	4062	0.72%	40570	7.17%
11	5491	0.97%	28305	5.01%
12	4118	0.73%	51556	9.12%
13	12947	2.29%	13241	2.34%
14	10009	1.77%	28254	5.00%
15	14666	2.59%	13479	2.38%
16	14154	2.50%	24955	4.41%
17	9171	1.62%	16194	2.86%
18	15813	2.80%	36802	6.51%
19	11287	2.00%	18755	3.32%
20	7009	1.24%	18612	3.29%
21	10887	1.93%	22517	3.98%
22	12000	2.12%	17412	3.08%
23	17190	3.04%	16294	2.88%
24	10736	1.90%		
25	13934	2.46%		
26	11993	2.12%		
27	18957	3.35%		
28	16944	3.00%		
29	12581	2.22%		
30	11999	2.12%		
31	13171	2.33%		
32	13934	2.46%		
33	10912	1.93%		
34	16626	2.94%		
35	10499	1.86%		
36	13066	2.31%		
AVE		**2.03%**		**4.20%**
STD DEV		**0.87%**		**1.79%**

Table 5-3 Crack density for samples cured at high temperature

	HT1	HT1	HT2	HT2	HT3	HT3
IMAGE #	TOTAL CRACK LENGTH μm	CRACK DENSITY μm/μm^2	TOTAL CRACK LENGTH μm	CRACK DENSITY μm/μm^2	TOTAL CRACK LENGTH μm	CRACK DENSITY μm/μm^2
1	7492	1.32%	23468	4.15%	4826	0.85%
2	5984	1.06%	15225	2.69%	7101	1.26%
3	10471	1.85%	9406	1.66%	5597	0.99%
4	1690	0.30%	13244	2.34%	7318	1.29%
5	N/A		15067	2.66%	N/A	
6	4028	0.71%	17956	3.18%	1367	0.24%
7	5131	0.91%	15565	2.75%	2085	0.37%
8	4549	0.80%	23055	4.08%	5407	0.96%
9	5261	0.93%	16544	2.93%	1323	0.23%
10	5569	0.98%	14729	2.60%	2099	0.37%
11	2422	0.43%	11580	2.05%	2512	0.44%
12	3485	0.62%	13282	2.35%	2351	0.42%
13	7492	1.32%	13930	2.46%	4826	0.85%
14	5213	0.92%	11125	1.97%	N/A	
15	3445	0.61%	12155	2.15%	1737	0.31%
16	2303	0.41%	9297	1.64%	1761	0.31%
17	4778	0.84%	13067	2.31%	1488	0.26%
18	1860	0.33%	6916	1.22%	2613	0.46%
19	4217	0.75%	18251	3.23%	2084	0.37%
20	3883	0.69%	13350	2.36%	1051	0.19%
21	4234	0.75%	8304	1.47%	N/A	
22	4811	0.85%	12628	2.23%	N/A	
23	6452	1.14%	15814	2.80%	N/A	
24	1847	0.33%	26698	4.72%	2073	0.37%
25	2740	0.48%	30150	5.33%	1633	0.29%
26	4085	0.72%	13925	2.46%	1018	0.18%
27	3847	0.68%	16701	2.95%	1127	0.20%
28	3830	0.68%			852	0.15%
29	4222	0.75%			1613	0.29%
30	6181	1.09%			1329	0.23%
31	N/A				2242	0.40%
32	2740	0.48%			1633	0.29%
33					1938	0.34%
34					3003	0.53%
35					2069	0.37%
AVE		**0.79%**		**2.69%**		**0.46%**
STD DEV		**0.34%**		**0.95%**		**0.31%**

Table 5-4 Crack density for samples cured at room temperature

	RT1	RT1	RT2	RT2	RT3	RT3
IMAGE #	TOTAL CRACK LENGTH μm	CRACK DENSITY $\mu m/\mu m^2$	TOTAL CRACK LENGTH μm	CRACK DENSITY $\mu m/\mu m^2$	TOTAL CRACK LENGTH μm	CRACK DENSITY $\mu m/\mu m^2$
1	10678	1.89%	6200	1.10%	13046	2.31%
2	8037	1.42%	3130	0.55%	20037	3.54%
3	7662	1.35%	2734	0.48%	13751	2.43%
4	7844	1.39%	3066	0.54%	18069	3.20%
5	4864	0.86%	3535	0.63%	NA	
6	4460	0.79%	2941	0.52%	25207	4.46%
7	5308	0.94%	6938	1.23%	14350	2.54%
8	4740	0.84%	4607	0.81%	12386	2.19%
9	3957	0.70%	5340	0.94%	17159	3.03%
10	2305	0.41%	8500	1.50%	16620	2.94%
11	1414	0.25%	8500	1.50%	13105	2.32%
12	3001	0.53%	5800	1.03%	14599	2.58%
13	10678	1.89%	6200	1.10%	22820	4.04%
14	2193	0.39%	5851	1.03%	20047	3.55%
15	928	0.16%	10292	1.82%	16108	2.85%
16	5708	1.01%	4244	0.75%	18213	3.22%
17	2645	0.47%	7785	1.38%	16839	2.98%
18	3161	0.56%	5769	1.02%	28603	5.06%
19	3560	0.63%	5348	0.95%	11560	2.04%
20	4524	0.80%	9562	1.69%	22714	4.02%
21	2316	0.41%	5424	0.96%	16569	2.93%
22	3484	0.62%	18091	3.20%	7182	1.27%
23	7554	1.34%	13235	2.34%		
24	4942	0.87%	12085	2.14%		
25	4041	0.71%	10144	1.79%		
26	5291	0.94%	17788	3.15%		
27	5646	1.00%	14878	2.63%		
28	4701	0.83%	25652	4.54%		
29	5441	0.96%	18797	3.32%		
30	4958	0.88%	15203	2.69%		
31	3778	0.67%	7651	1.35%		
32	4041	0.71%	10144	1.79%		
33	6235	1.10%	8199	1.45%		
34	3822	0.68%	5442	0.96%		
35	7610	1.35%	17262	3.05%		
AVE		**0.83%**		**1.60%**		**3.02%**
STD DEV		**0.39%**		**0.97%**		**0.88%**

Table 5-5 Average crack density for oven-dried and non-dried samples

Sample	Crack density ($\mu m/\mu m^2$)
95B00P ODHT-1	2.03%
95B00P ODHT-2	4.20%
Average	**3.12%**
95B00P ODRT-1	2.00%
95B00P ODRT-2	3.43%
Average	**2.72%**
95B00P HT-1	0.79%
95B00P HT-2	2.69%
95B00P HT-3	0.46%
Average	**1.32%**
95B00P RT-1	0.83%
95B00P RT-2	1.60%
95B00P RT-3	3.02%
Average	**1.82%**
Average Oven-dried samples	**2.92**
Average Non-dried samples	**1.57**

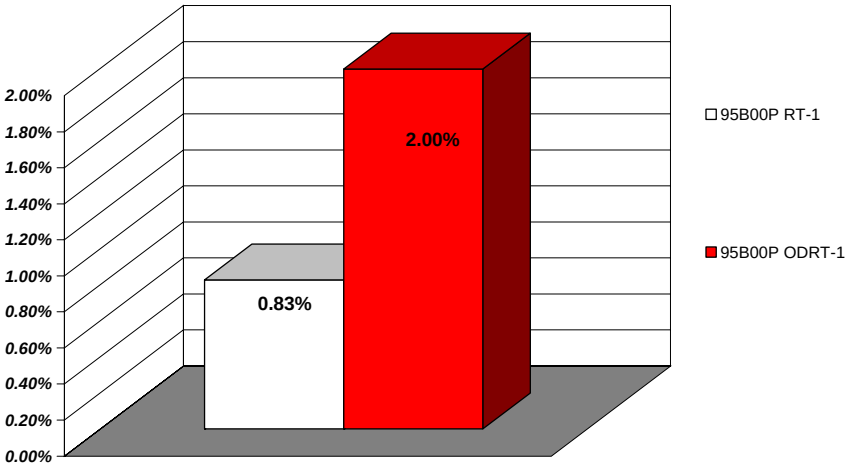

Figure 5-1 Microcrack density comparison of oven-dried and non-dried samples cured at room temperature

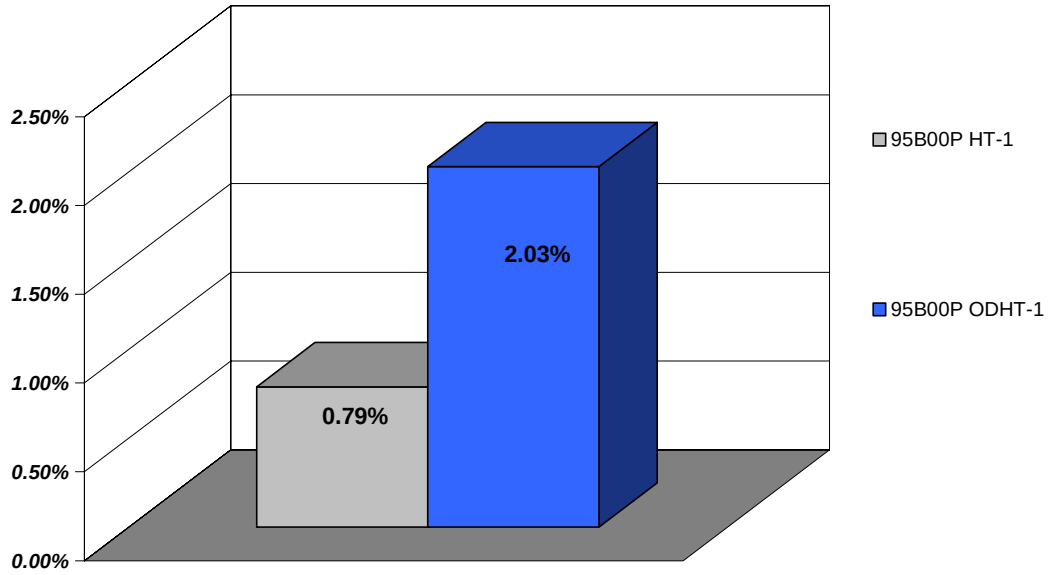

Figure 5-2 Microcrack density comparison of oven-dried and non-dried samples cured at high temperature

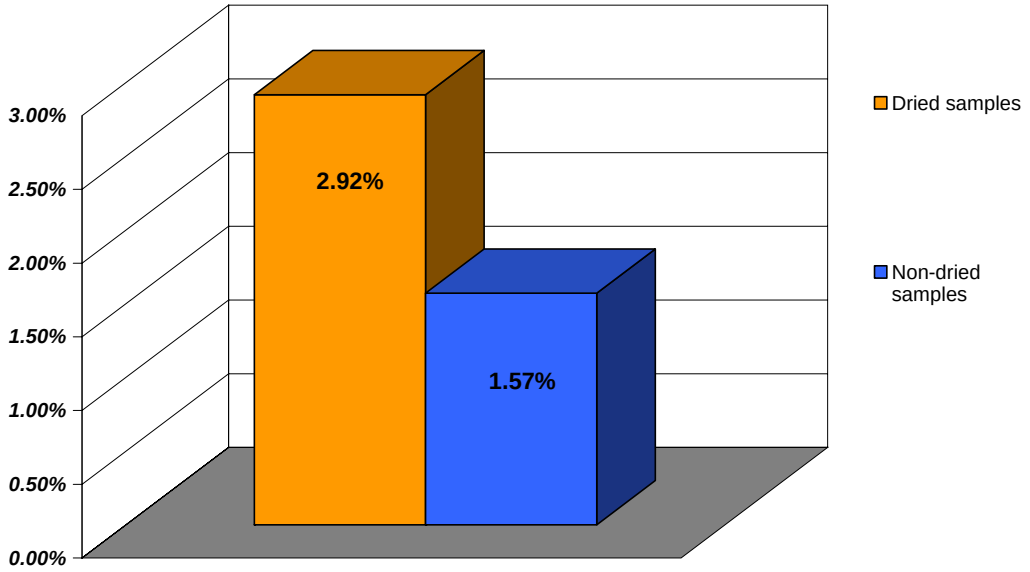

Figure 5-3 Microcrack density comparison of dried samples and non-dried samples

Effects of High Curing Temperature

Table 5-5 and Figure 5-4 show average crack densities of samples cured at room and high temperatures. The analysis revealed no significant difference between microcrack densities of samples of concrete cured at room temperature and those cured at elevated temperature. The results do not provide conclusive evidence as to the effects of high temperature curing on the development of microcracks in mass concrete.

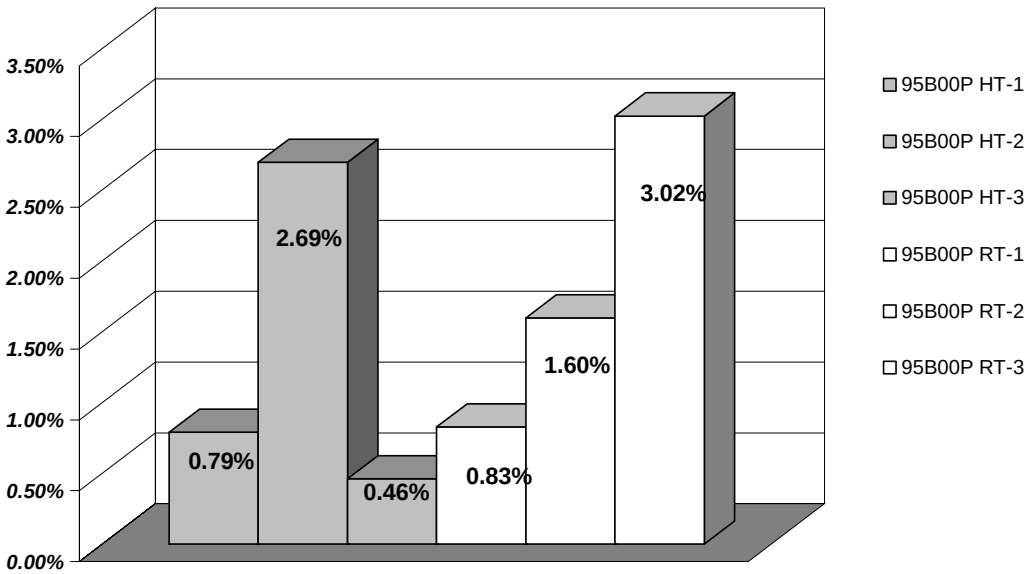

Figure 5-4 Microcrack density comparison of samples cured at room and high temperatures

CHAPTER 6

SUMMARY, CONCLUSIONS AND RECOMMENDATIONS

Summary

The objective of this research project was to determine if high temperatures during curing of concrete cause microcracks in the concrete matrix. In addition, the method for preparing concrete samples for microscopic study was tested for accuracy in the detection and quantification of microcracks in the concrete samples cured at elevated temperatures. The following is a summary of the experimental procedure and analysis of this study.

A literature review was conducted to identify industry practices for sample preparation in microscopy analysis. Research papers related to the detection and quantification of microcracks in concrete were evaluated for determination of the resources needed to implement the techniques for conducting this study. Previous image analysis procedures used to analyze SEM-generated images were studied for the electronic quantification and detection of microcrack lengths and densities. The literature review showed that several techniques for sample preparation exist, some of which require equipment resources that are out of the scope of this project, as well as techniques that undermine the requirements for the study of *in-situ* properties of concrete. The techniques which presented the least destructive preparation steps were used for the project.

The image analysis procedures were developed based on previous research project criteria, as well as the tools and capabilities of the imaging software acquired to conduct the image analysis. The literature review showed that there are no standard techniques for sample preparation for the intent of analyzing microcracks in concrete with complete assurance that the procedure does not induce secondary cracking. The *in-situ* study of concrete microstructure is an area of great debate because of physical constraints in the cutting and grinding preparation process. However, it was estimated that the preparation procedures used for this study represented the most suitable process given the constraints in time, budget, and equipment availability.

The first step in the experimental process was to determine if the sample preparation technique utilizing the epoxy impregnation and grinding and polishing processes were inducing additional cracks into the concrete. Furthermore the conditions found in the microscopy generated images for these samples closely resembled the conditions of the concrete in place. Secondly, once the technique was verified, additional samples would be prepared to provide a larger amount of images and data to test the hypothesis of microcrack generation from high temperature levels during curing.

The specimens selected for the study were chosen from the batch of concrete mixes which produced the highest levels of heat of hydration as well as the highest total temperature levels during curing. Two sets of samples were paired for comparison of temperature conditions during curing. For each sample cured at high temperature, a regular temperature sample was also prepared as a control specimen. The percentage of cracks in each sample, high temperature and regular temperature, for the same concrete sample mix were then compared for microcrack concentration.

The images generated from each sample were analyzed with a commercial microscopy imaging computer program that would output the quantity of cracks found in the image field area. The criterion used for the differentiation of cracks from voids and other concrete matrix features was established to control the effects of user bias in the quantification process. It is important to keep in mind that the image areas viewed at the 150X magnification levels represent an image field of 650 microns by 870 microns. The scanned image field represented a minimal 1% of the prepared concrete sample surface. This is a limitation that has inevitable time resource constraints due to the limited image areas scanned, the finite amount of images that can be individually analyzed, as well as the ability to capture and quantify microcracks at a minimum SEM magnification level, which ultimately determines the viewable image field area.

Conclusion

The following conclusions can be stated after the analysis of the results from the image analysis methodology. The procedure for sample preparation was tested against a crack-induced set of samples to validate the sample preparation technique. Figure 6-1 shows the average crack densities obtained from the image analysis of the three pair of samples tested for validity of technique. The values shown in Figure 6-1 are the average crack densities for the three oven-dried samples and the three non-oven-dried samples.

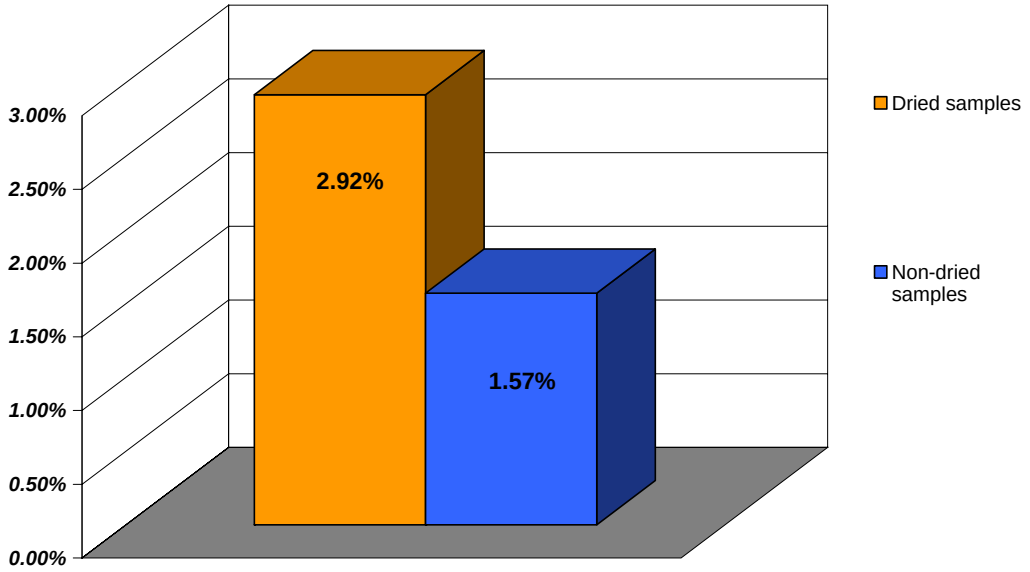

Figure 6-1 Microcrack density comparison of pre-dried samples and non-dried samples

The samples that induced drying shrinkage cracks displayed approximately 86% more cracks than the non-dried samples. Figure 6-2 and Figure 6-3 illustrate the cracks quantified in an oven-dried sample (Figure 6-2) and a non-oven-dried sample (Figure 6-3).

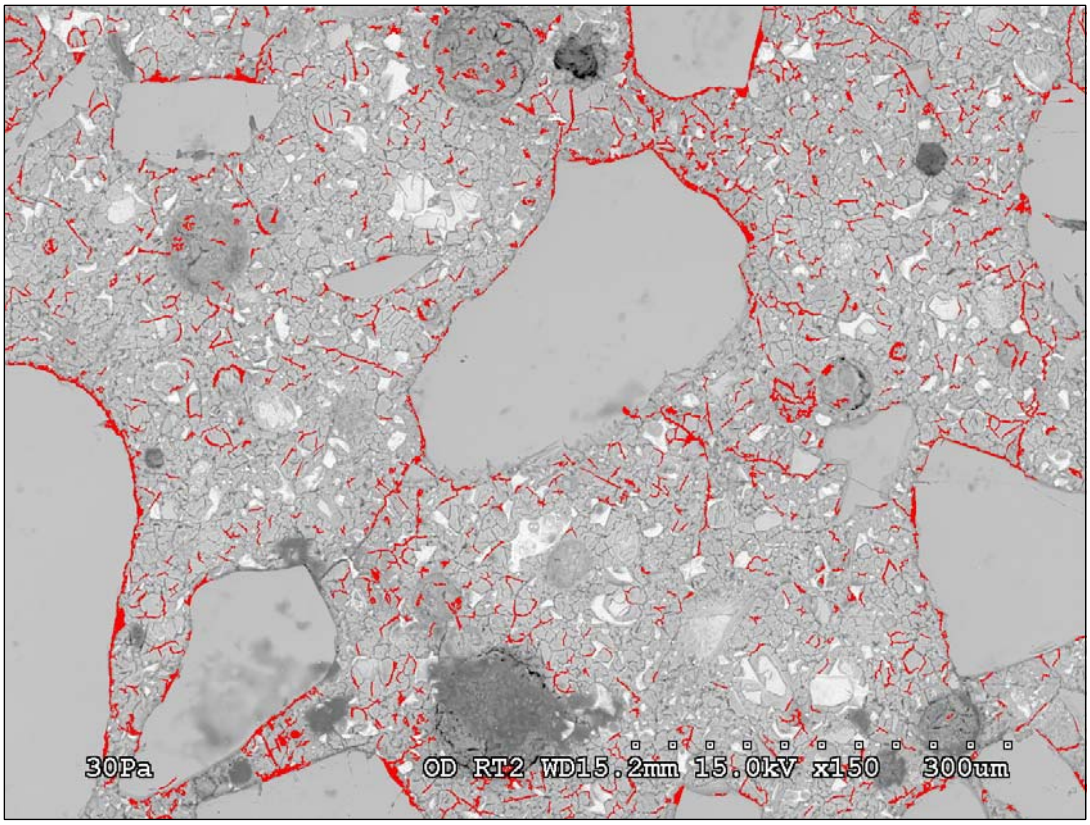

Figure 6-2 Microcracks in Oven-dried sample

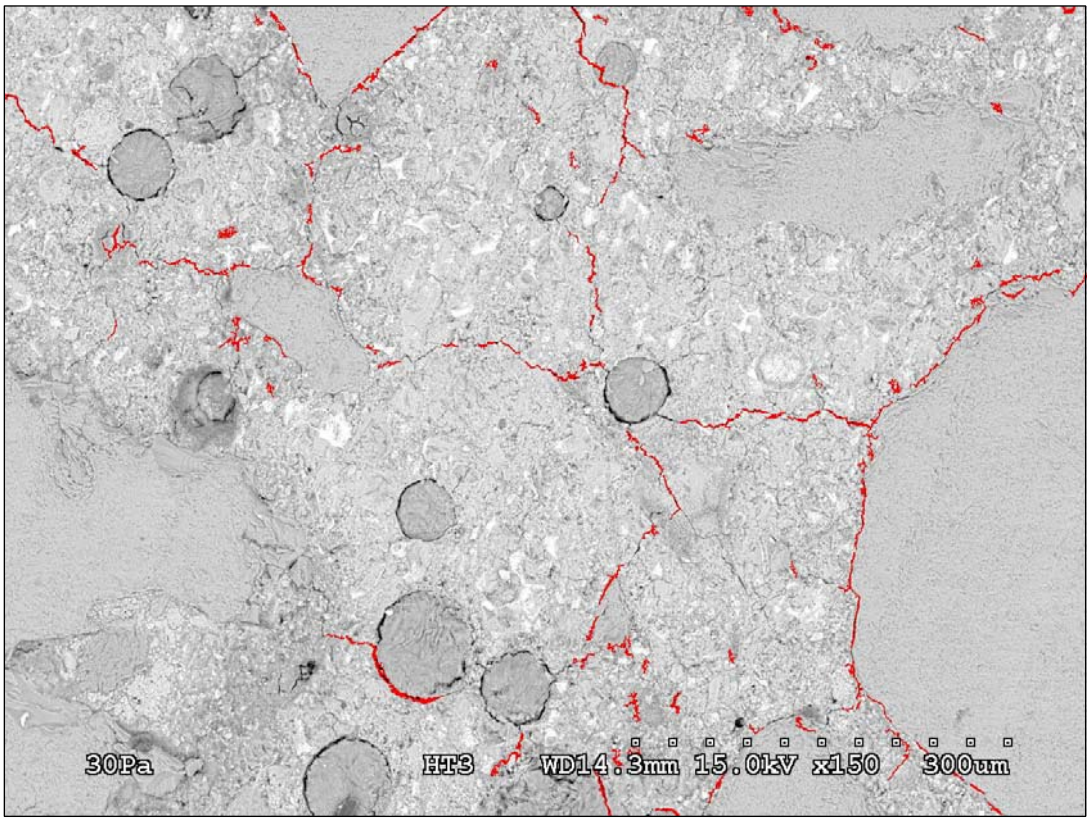

Figure 6-3 Microcracks in non-oven-dried sample.

After having verified the sample preparation technique, the task of evaluating the crack concentration in samples cured at elevated temperatures against those cured at room temperature was set forth. The research revealed that no correlation exists between concrete curing temperature and the concentration of microcracks in the concrete. Figure 6-4 below shows the results for the average crack densities obtained from the six samples used in this study.

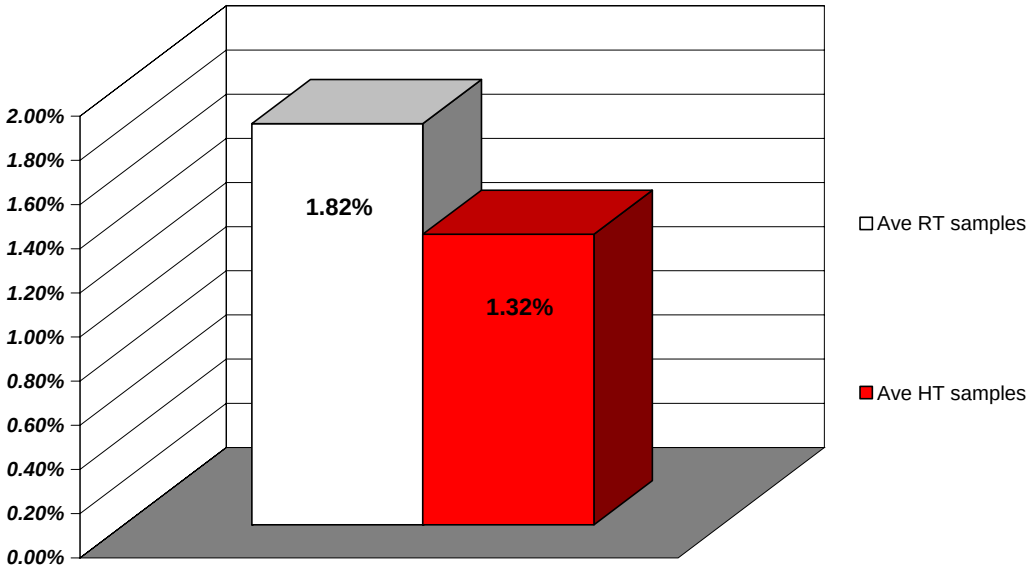

Figure 6-4 Microcrack density comparison for high temperature and room temperature curing conditions.

The data obtained demonstrated no significant difference between the average crack densities for room temperature cured samples (RT) and the high temperature cured samples (HT). Therefore, based on the aforementioned findings it can be concluded that for the samples tested in this experiment the temperature levels reached during mass concrete curing did not influence the formation of microcracks in the concrete structure.

There are several factors that are noteworthy regarding the validity of these findings. The factors are the following:

- Control of manual grinding and polishing processes
- Exposure to heat during epoxy impregnation

- Bias in crack identification
- Variation in grayscale properties between images and its influence in crack identification results
- Percentage of concrete surface area studied

Recommendations

The results of this study show that for the samples tested in this project the current quality control procedures required by the FDOT to control temperature differentials in mass concrete pours should be sufficient for preventing the formation of microcracks in concrete structures. The following recommendations are made for conducting future work in this area of study:

- Samples with different cementitious material content can be tested for crack formation, and compared to the different fly-ash, slag and Portland cement mix ratios.
- During the grinding stages of sample preparation a method to control the pressure applied to the grinding /polishing wheel should be considered. This can be achieved via the upgrade to a sample holder arm and pressure regulator apparatus to the MetPrep3 Grinder/Polisher machine.
- The ultra low viscosity kit proved to be very difficult to work with, in particular with the control of temperature and air entrainment into the epoxy mix. A simpler resin-hardener epoxy kit should be utilized which can be mounted at room temperature. The epoxy should also be mixed and impregnated via a vacuum pump chamber to accelerate the impregnation

process. The use of ethanol which dehydrates the concrete samples can be eliminated.

- A product equal or similar to the Epovac vacuum impregnation apparatus by Struers, Inc. would suffice for the preparation of epoxy impregnated samples.

LIST OF REFERENCES

American Concrete Institute (ACI) Committee 116, Report SP-19, Farmington Hills, Michigan, 1995

American Concrete Institute (ACI) Committee Manual of Concrete Practice, Report 207.2R-95, "Effect of Restraint, Volume Change, and Reinforcement on Cracking of Mass Concrete", Farmington Hills, Michigan, 2003

American Concrete Institute (ACI) Committee Manual of Concrete Practice, Report 207.1R-96, "Mass Concrete", Farmington Hills, Michigan, 2003

Advances in Materials Problem solving with Electron Microscope - Proceedings of Material Research Society, Volume 589, 1999

Ammouche, A. Breysse, D. Hornain, H. Didry, O., and Marchand, J., "New image analysis technique for the quantitative assessment of microcracks in cement-based material," Cement and Concrete Research Volume 30, No.1, Page 25-35, 2000

Ammouche, A., Riss J., Breysse D., and Marchand, J., "Image Analysis for the Automated Study of Microcracks in Concrete", Cement and Concrete Composites, Vol. 23, pp. 267-278, 2001

Bisschop, J., and Van Mier, J.G.M., "How to study drying shrinkage microcracking in cement-based materials using optical and scanning electron microscopy," Cement and Concrete Research Volume 32, No. 2, Page 279-287, February 2002

Chini, A. and Parham A., "Adiabatic Temperature Rise of Mass Concrete in Florida", Report to the Florida Department of Transportation, Gainesville, Florida, 2004

Darwin, D., Abou-Zeid, M.N., and Ketchman, K.W., "Automated Crack Identification for Cement Paste", Cement and Concrete Research Vol. 25, No.3, pp. 605-616, 1995

Detwiler, R.J., Powers, L.J., Hjorth, U., Ahmed, W.U., Srivener, K.L., and Kjellsen, K.O., "Preparing Specimens for Microscopy", Concrete International, Vol. 23, No. 11, pp. 51-58, November 2001

Florida Department of Transportation, Structural Design Guide, Section 3.9 Mass Concrete, Tallahassee, Florida

Gran, H. C., "Fluorescent liquid replacement technique: A means of crack detection and water-binder ratio determination in high-strength concretes." Cement and Concrete Research Volume 25, No 5, Page 1063-1074, 1995

Hanke, L. Variable Pressure Scanning Electron Microscopy for Nonconductive and Volatile Samples, Handbook of Analytical Methods, 1999

Hornain H., Marchand J., Ammouche A., Commene J.P., and Moranville M., "Microscopic observation of cracks in concrete-a new sample preparation technique using dye impregnation." Cement and Concrete Research, Volume 26, No.4 Page 573-583, 1996

Kjellsen, K. O., and Jennings, H M., "Observations of microcracking in cement paste upon drying and rewetting by environmental scanning electron microscopy," Advanced Cement Based Materials Volume 3, No.1, Page 14-19, January 1996

Knab L.I., Walker H.N., Clifton J.R., and Fuller E.R., "Fluorescent thin sections to observe the fracture zone in mortar," Cement and Concrete Research, Volume 14, No. 3, Page 339-344, 1984

Maggenti R., Mass Concrete Report, San Francisco-Oakland Bay Bridge East Spans Safety Project. 04-Ala/SF-80-Var, E.A. 04-012021, Available online at http://www.dot.ca.gov/hq/esc/tollbridge/SFOBB/EastSpan/012024/MaterialsHandout/cd2/concret1.pdf, last seen, Oct 12, 2004

Marusin S., "Sample preparation-the key to ESM studied of failed concrete," Cement and Concrete. Composites Volume 17, No.4, Page 311–318, 1995

Nemati, K.M., "Fracture Analysis of Concrete Using Scanning Electron Microscopy," Scanning, The Journal of Scanning Microscopies, Vol. 19, No. 6, pp. 426-430, Sept. 1997

Nemati, K.M., and Stroeven, P., "Stereological Analysis of Micromechanical Behavior of Concrete", Materials and Structures, RILEM, Vol. 34, No. 242, pp. 486-494, October 2001

Najjar, W.S., Aderhold, H.C., and Hover, K.C., "Application of neutron radiography to the study of microcracking in concrete Cement", Concrete and Aggregates, Volume 8, No. 2, Page 103-109, 1986

Oberholster, R. E., Maree, H. and Brand, J. H. B, "Cracked prestressed concrete railway sleepers: alkali silica reaction or delayed ettringite formation," Proceedings of the 9th International Conference on Alkali-Aggregate Reaction in Concrete, London, Page 740-749, 1992

Ollivier, J.P., Cement and Concrete Research, Volume 15, No.6, Page 1055-1060, 1985

Patel, H.H., Bland, C.H., and Poole, A.B., "Microstructure of concrete cured at elevated temperatures," Cement and Concrete Research Volume 25 No. 3 Page 485-490, April 1995

Perkes, P., ACEPT W group, Department of Physics and Astronomy, Arizona State University, http://acept.la.asu.edu/PiN/rdg/elmicr/elmicr.shtml Last Visited October 2004

Ringot, E., and Bascoul, A., "About the analysis of microcracking in concrete," Cement and Concrete Composites Volume 23, No. 2-3, Page 261-266, April 2001

Samaha, H.R., and Hover, K.C., "Influence of microcracking on the mass transport properties of concrete," ACI materials Journal, Volume 89, No.4, Page 416-424, 1992

Slate, F.O., and Hover, K.C., Fracture Mechanics of Concrete: Edited by F.H. Whitmann, Published by Elsevier Science Page 85-93, 1984.

Slate F.O., and Olsefski, S., "X-Rays for Study of Internal Structure and Microcracking of Concrete," Journal of American construction Institute, Volume 60, No. 5, Page 575-588, 1963

Soroushian, P., Elzafraney, M., and Nossoni, A., "Specimen preparation and image processing and analysis techniques for automated quantification of concrete microcracks and voids," Cement and Concrete Research Volume 33, No.12, Page 1949-1962, December 2003

Saint John, D., Poole A., and Sims A, Concrete Petrography-A Handbook of Investigative Techniques Published by Arnold, 1998

Struble L. J., and Stutzman P.E., "Epoxy impregnation of hardened cement for microstructural characterization," Journal of Material Science Letters, Volume 8, Page 632-634, 1989

Stutzman P, Scanning Electron Microscopy in Concrete Petrography, Materials Science of Concrete Special Volume: Calcium Hydroxide in Concrete (Workshop on the Role of Calcium Hydroxide in Concrete). Proceedings of The American Ceramic Society, edited by J. Skalny, J. Gebauer and I. Odler, November 1-3, 2000, Anna Maria Island, Florida, Page 59-72, 2001

Stutzman, P.E., and Clifton, J.R., "Specimen Preparation for Scanning Electron Microscopy", Proceedings from the Twenty-First International Conference on Cement Microscopy, April 25-29, 1999, Las Vegas, NV, pp. 10-22., 1999

Wang, X., Wu B., and Wang, Q., "Online SEM Investigation of Microcrack Characteristics of Concretes at Various Temperatures", Cement and Concrete Research, Vol. 35, No. 7, pp. 1385-1390, July 2005